

See discussions, stats, and author profiles for this publication at: <https://www.researchgate.net/publication/263953889>

# Charge Photogeneration in Neat Conjugated Polymers

ARTICLE *in* CHEMISTRY OF MATERIALS · OCTOBER 2013

Impact Factor: 8.35 · DOI: 10.1021/cm4027144

CITATIONS

25

READS

57

5 AUTHORS, INCLUDING:



**Obadiah G. Reid**

University of Colorado Boulder

27 PUBLICATIONS 914 CITATIONS

SEE PROFILE



**Ryan D. Pensack**

Princeton University

25 PUBLICATIONS 367 CITATIONS

SEE PROFILE



**Yin Song**

University of Michigan

12 PUBLICATIONS 250 CITATIONS

SEE PROFILE



**Garry Rumbles**

National Renewable Energy Laboratory

209 PUBLICATIONS 6,421 CITATIONS

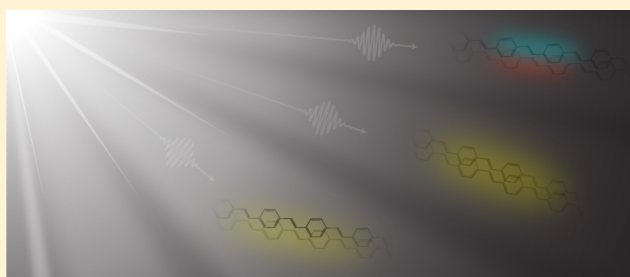
SEE PROFILE

## Charge Photogeneration in Neat Conjugated Polymers

Obadiah G. Reid,<sup>†</sup> Ryan D. Pensack,<sup>‡</sup> Yin Song,<sup>‡</sup> Gregory D. Scholes,<sup>‡</sup> and Garry Rumbles<sup>\*,†,§</sup><sup>†</sup>Chemical and Materials Science Center, National Renewable Energy Laboratory, 15013 Denver West Parkway, Golden, Colorado 80401, United States<sup>‡</sup>Department of Chemistry, University of Toronto, 80 St. George Street, Toronto, Ontario M5S 3H6, Canada<sup>§</sup>Department of Chemistry and Biochemistry, University of Colorado at Boulder, Boulder, Colorado 80309, United States

**ABSTRACT:** The origin and yield of charges in neat conjugated polymers has long been controversial. In this paper, we review the body of literature that has been created over the past three decades of research in this field and provide insight from our own recent work highlighting the importance of polymer microstructure in understanding the photophysics of these materials. We focus primarily on polythiophene, poly(*p*-phenylene vinylene), and ladder-type poly(*p*-phenylene) derivatives, as these three prototypical polymer backbone structures have undergone the most complete study. We find compelling evidence that the primary photoexcitations in conjugated polymers include both intrachain excitons and excimers, that charges are produced in a secondary process, primarily from breakup of intrachain excitons, and that the locus of long-lived charge generation is at the interface between amorphous and crystalline domains of the polymer. Interestingly, the existence of interchromophore complexes that we refer to as excimers has largely been ignored in the development of organic photovoltaics based on conjugated polymers. We suggest that the prevalence of this species may help explain certain mysterious features in that body of work, in particular the excess energy offset required for efficient charge separation in donor/acceptor blends and the requirement for intimately mixed phases of the two materials for maximally efficient photocurrent generation.

**KEYWORDS:** excimer, polaron, exciplex, microwave conductivity, transient absorption, pump–probe, pump–dump



## ■ INTRODUCTION

The origin of photogenerated charges in neat (i.e., without an added electron or hole acceptor) conjugated polymers has long been controversial. Initially, there was debate over whether the primary photoexcitation was an interband transition which directly produced free carriers,<sup>1–5</sup> or a local excitation known as a Frenkel exciton.<sup>6–9</sup> A preponderance of evidence has since shown the latter to be the case. Nevertheless, charges are generated upon photoexcitation of these materials,<sup>10–13</sup> and a complete description of this process has never been achieved.

In this perspective, we describe the key results that lead to the molecular, excitonic picture and proceed to discuss charge generation within this framework. We emphasize the influence of interchain species, such as excimers, and the confusion their presence has sometimes engendered. It will become clear that distinguishing between different interchain species is not trivial. In this context we describe our recent contributions, showing on the one hand the potential of two-dimensional electronic spectroscopy to distinguish different types of excited-state species and on the other how microwave photoconductivity experiments reveal the influence polymer microstructure has on free charge generation.<sup>14,15</sup> In addition, we attempt to make explanatory connections between present mysteries in organic photovoltaics and the ubiquitous presence of interchain species which are not often discussed.

We begin with a discussion of excited-state terminology, particularly relevant to how we approach the topic of interchain excitations.

## ■ EXCITED-STATE TERMINOLOGY AND INTERCHAIN SPECIES

A wide variety of nomenclature is used to describe the excited species present in conjugated polymer films, in part because we are using discrete terms to describe a continuum of charge separation and electronic delocalization. Nevertheless, these categories are important and we think it useful to provide precise definitions.

We begin with the “exciton”.<sup>16</sup> There are two kinds of excitons discussed for conjugated polymers: along the chain or between chains. Excitons between chain chromophores are typical Frenkel excitons, that is, the collective excited states are linear combinations of electronic excitations of each chromophore in the aggregate. We describe these Frenkel excitons in some more detail later in this paper. Excitons along the chain refer to the chromophore unit defined by the extended  $\pi$ -

**Special Issue:** Celebrating Twenty-Five Years of Chemistry of Materials

**Received:** August 11, 2013

**Revised:** September 22, 2013

**Published:** September 24, 2013



conjugation—limited mainly by conformational disorder. Owing to the importance of orbital overlap, a simple Frenkel model is insufficient to describe these delocalized excited states, so detailed treatments using quantum chemical methods are required.<sup>17</sup> In the present paper, we use the term *exciton* to refer to the intrachain electronic excited state (whether singlet or triplet) with its associated molecular and lattice distortions,<sup>18</sup> the inclusion of which is taken for granted in the following definitions.

An “excimer”, in contrast, is an interchain excited-state species where the frontier orbital electron density is shared equally between neighboring chromophores (conformational subunits) that are nominally identical. The key distinguishing features of excimers are that (a) they are formed by geometrical relaxation after photoexcitation and (b) the electronic coupling that stabilizes them is strong and involves orbital overlap. This latter property is important in considering the transition to a polaron pair because the primary orbital overlap-dependent interactions that augment the Coulombic coupling between transition densities are described in valence bond terms as a resonance between charge-transfer configurations.<sup>19–21</sup>

In an excimer, the basis configurations describing the excited states of molecules A and B mix by electronic coupling. These basis configurations provide a formally equivalent description of the electronic excitations as the CI-singles method in the molecular orbital basis. The configurations are the locally excited configurations  $A^*B$  and  $AB^*$  (the prime denotes electronic excitation) and charge transfer configurations  $A^+B^-$  and  $A^-B^+$  (see Figure 2 of ref 22).

Strictly speaking, excimers possess a repulsive ground state and are not accessible by direct excitation. They form only in the excited state through the attractive interaction between one chromophore in the excited state and another in the ground state. However, the crowded solid-state environment of a conjugated polymer film complicates this picture. Preassociation of the excimer may take place in the ground state due to how the polymer chains pack in films. These “pre-associated excimers” are, however, not identical to “aggregates”, which, although they are quite similar to excimers in the configuration of the excited state, have an attractive ground state potential energy surface and corresponding structured absorption and emission features. The primary consequence of this preassociation of chromophores, aside from the appearance of aggregates, is that excimers may form on an ultrafast time scale, whereas in the traditional picture excimer formation is controlled by chromophore diffusion. We note that, in addition to the above-mentioned processes, electronic energy transfer may occur to sites at which excimers form.

An “exciplex” is an excitation where frontier orbital electron density is shared unequally between two dissimilar chromophores. The definition here is identical to the excimer except for the asymmetric weighting of the electron density, and similar complications to the traditional definition apply in solid-state films. Moreover, it is evident that these definitions referring to only a pair of chromophores, particularly for the excimer, must be generalized to include the possibility that excitations may be shared across many chain segments.

Finally, we define “polarons” as the case of an excimer or exciplex where nuclear reorganization stabilizes one of the charge-transfer configurations. This “lattice” (or polarization) deformation is a key feature of the polaron model. Physically it means that the free energy of the complex is lowered most by localizing charges (or excitation) and strongly reorganizing the

bath of nuclear degrees of freedom rather than sharing the bath reorganization around a charge-transfer resonance. A classic example of this kind of bath-induced symmetry breaking is 9,9'-bianthryl. This symmetric anthracene dimer shows normal anthracene-like fluorescence in nonpolar solvents, but fluorescence indicative of a symmetry-breaking charge-transfer state in polar solvents.<sup>23–26</sup> Polarons, therefore, cannot be defined solely on the basis of an electronic level diagram—the nuclear coordinate must also be considered because the coefficients defining the admixture of  $A^*B$ ,  $AB^*$ ,  $A^+B^-$ , and  $A^-B^+$  in the wave function depend sensitively on the nuclear configuration (intramolecular geometry as well as polarization of the environment).

Finally, it is not absolutely clear that a polaron pair bound by their mutual coulomb attraction ought to be considered as a charged species. Rather, it is a dipole. Thus, in this review we limit the term “charge” to the subset of polarons that are mobile, able to contribute to photoconductivity at low electric fields.

It should be clear to the reader that the distinction between excimers, exciplexes, and bound polaron pairs is not necessarily an easy one to make experimentally. These categories represent a continuum of charge separation, and they may behave quite similarly in certain experiments. All of them are expected to have weak coupling with the ground state, all of them ought to dissociate into free charge under sufficiently high electric fields, and they are expected to possess very similar transient absorption spectra.<sup>27,28</sup> It is with this difficulty in mind that we approach the question of “charge” photogeneration in neat conjugated polymers.

## ■ PRIMARY PRODUCT(S) OF PHOTOEXCITATION

The initial controversy over the nature of primary photoexcitations in conjugated polymers focused on whether a semiconductor band picture or a molecular picture is most appropriate to describe the electronic structure of these materials.

Evidence for an interband transition came primarily from the ultrafast, <100 fs, appearance of both photoconductivity<sup>4</sup> and subgap photoinduced absorption (PA)<sup>2,3</sup> bands near 1.5 and 0.5 eV<sup>29</sup> in poly(*p*-phenylene vinylene) (PPV) that were uncorrelated with stimulated emission (SE) or photoluminescence (PL) dynamics. In addition, both steady-state and transient photoconductivity was found to be temperature independent.<sup>1</sup> Instantaneous polaron yields of >10% were reported for a variety of conjugated polymers.<sup>2,3,30</sup>

In evaluating this evidence, it is important to consider the potential effects of second-order processes, which are very difficult to avoid in pump–probe experiments because of the high photon density that is often required for sufficient signal-to-noise ratio, and the high peak power inherent to very short optical pulses, even at low average power.<sup>31</sup> This is particularly true of some of the seminal literature. Recently, progress has been made both in understanding the threshold for second order processes and in performing experiments that avoid or account for this complication. Gélinas et al., for example, recently carried out a careful analysis of time-resolved photoluminescence measurements on poly(9,9'-dioctylfluorene-co-benzothiadiazole) (F8BT) that showed high-order effects to occur in neat films of F8BT down to  $\sim 1 \mu\text{J cm}^{-2}$  as evinced by an accelerated stimulated emission decay from  $\sim 1$  ns at  $1 \mu\text{J cm}^{-2}$  to  $\sim 100$  ps at  $10 \mu\text{J cm}^{-2}$ .<sup>32</sup> The accelerated decay of the singlet photoluminescence at  $10 \mu\text{J cm}^{-2}$  was

attributed to exciton-charge quenching. Piris et al. similarly were able to avoid high-order effects in films of poly(3-hexylthiophene) (P3HT) at a fluence of  $<1 \mu\text{J cm}^{-2}$ .<sup>33</sup> Gulbinas et al. found the absence of nonlinear relaxation processes at a fluence of  $\sim 10 \mu\text{J cm}^{-2}$  in films of MeLPPP.<sup>34</sup> Nevertheless, it is not uncommon for researchers to operate at a slightly higher threshold whereby it was shown, for example, that  $\sim 50\%$  of device external quantum efficiency (relative to continuous-wave conditions) is retained at  $\sim 10\times$  the optimally low fluence.<sup>35</sup> We have made an attempt in this perspective to highlight work performed at relatively low fluence,  $\sim 10 \mu\text{J cm}^{-2}$  or below, and we comment on the potential effects of second-order processes where appropriate.

In the present context, second-order processes are important. Subpicosecond appearance of photoconductivity in ultrafast, high pump fluence, experiments can be explained readily by sequential excitation<sup>36</sup> to higher lying states with substantial charge-transfer character.<sup>37,38</sup> Additional fast, high efficiency, charge generation in the picosecond time scale can likewise be ascribed to exciton–exciton annihilation (EEA) processes which, again, lead to higher lying excited states from which charge separation efficiency is enhanced.<sup>39,40</sup>

Subpicosecond appearance of PA in pump–probe measurements can, in part, be explained through the same second order processes as for photoconductivity. However, there is the additional complication that the PA bands induced by interchain species can be nearly identical to those expected for separated polarons.<sup>27,28,41</sup> For example, Vardeny and co-workers had previously claimed instantaneous production of charges in P3HT and poly[2-methoxy-5-(2-ethylhexyloxy)-1,4-phenylenevinylene] (MEH-PPV) with a yield of 30% and 10%, respectively, based on the ratio of the PA peak (at  $\sim 0.4$  eV in both polymers) assigned to polarons and that assigned to singlet excitons.<sup>30</sup> Since that publication, pressure-dependent PA studies by the same group have shown that, in fact, the ultrafast appearance of the PA band near 0.4 eV in MEH-PPV originally ascribed to polarons is better accounted for as an excimer state.<sup>28</sup>

Thus, the primary observations that support the band picture for photoexcitations in conjugated polymers can be explained within the molecular exciton picture, if the presence of interchain species such as excimers is considered. In contrast, there are many experimental results that cannot be easily explained within the band picture. We present four examples.

First, the existence of both strongly luminescent and dark conjugated polymers such as PPVs and trans-poly(acetylene), respectively, is readily explained in a unified model by taking into account their molecular nature and, specifically, in accounting for electron–electron correlations.<sup>38</sup> In contrast, the band model neglects electron correlations<sup>42</sup> and requires ad-hoc treatment of these two very similar materials.<sup>43</sup> Second, a very large applied electric field is required to substantially enhance charge generation in PPVs and ladder-type poly(*p*-phenylene)s (LPPPs), which indicates a rather high binding energy of the primary photoexcitation, on the order of several hundred millielectronvolts, consistent with the formation of Frenkel excitons,<sup>8,34,44</sup> and similarly large binding energy is expected on theoretical grounds.<sup>6,38,45</sup> Third, field-induced fluorescence quenching has been shown to evolve on a picosecond time scale, indicative of exciton breaking through a delayed process, secondary to initial excitation.<sup>44</sup> Fourth and finally, terahertz photoconductivity experiments show very little charge generation on the picosecond time scale ( $<1\%$  for

MEH-PPV and P3HT) even though the experiments were done at relatively high fluence,<sup>46–48</sup> clearly inconsistent with efficient subpicosecond free charge generation.

Although it does not seem that free charges are directly produced by optical-gap excitation in the absence of second-order effects, evidence for the formation of a large population of an optically dark interchain species other than separated charges is compelling. This possibility was suggested early on by Rothberg and co-workers under the title “spatially indirect excitons” in order to explain the same ultrafast PA bands that Heeger and Moses ascribed to free polarons.<sup>49</sup> The case is this: in PPV, two PA bands with identical kinetics appear on a subpicosecond time scale: one near 1.5 eV and one near 0.5 eV. The strength of these bands varies with excitation wavelength and shows competition with concomitant stimulated emission assigned to the intrachain exciton. The rapid appearance and spectra of this species is inconsistent with the formation of triplet excitons via known intersystem crossing rates. Nor can it be explained entirely by free polarons, as the strength of the absorption relative to the stimulated emission would imply a much higher yield of carriers than is observed in photoconductivity experiments<sup>49</sup> and would be inconsistent with all the evidence noted above ruling out efficient charge photogeneration on subpicosecond time scales. These observations demand a fourth alternative species.

Subsequent work has identified this fourth species in a variety of conjugated polymers, under several different names: spatially indirect excitons,<sup>49</sup> bound polaron pairs,<sup>29,45,50–52</sup> interchain excitons,<sup>53</sup> excimers,<sup>28,54,55</sup> or charge-transfer excitons,<sup>28</sup> to name a few. As we described in the preceding section, these labels are not all synonymous, but discerning the difference between competing hypotheses can be quite difficult, often impossible on the basis of the specific experiments that are reported. Indeed, only a handful of experiments reported to date have the potential to definitively distinguish between these various possible interchain species. We discuss two of these studies in detail below, both of which indicate that the neutral excimer is dominant.

## ■ DISTINGUISHING BETWEEN INTERCHAIN SPECIES

Evidence for the ultrafast formation of excimers as opposed to polaron pairs in conjugated polymers with relatively high yield comes from a number of different experiments. First, work by Vardeny, which we mentioned briefly above, shows that the PA bands previously assigned to polarons are in fact associated with excimers in MEH-PPV,<sup>28</sup> leading to the reasonable suspicion that this might be true in other polymers as well. This conclusion arises from combined experimental and theoretical work comparing the spectral shift in absorption bands for excimers and polaron pairs in response to applied hydrostatic pressure (i.e., increased polymer chain proximity). While their absorption bands are nearly identical under standard conditions,<sup>27,28</sup> decreasing the polymer chain separation was predicted through theoretical calculations on a model dimer to blue-shift the absorption of an excimer, while that of a polaron pair would remain essentially unchanged. Transient absorption measurements in a diamond anvil cell with pressures  $>100$  kBar showed a strong blue-shift in the ultrafast PA bands in response to the applied pressure, whereas very little shift was observed in the steady-state PA spectrum arising from free polarons. These results are summarized in Figure 1a and b.

Combining these conclusions with the “polaron” yield estimated in previous work by the same group suggests that



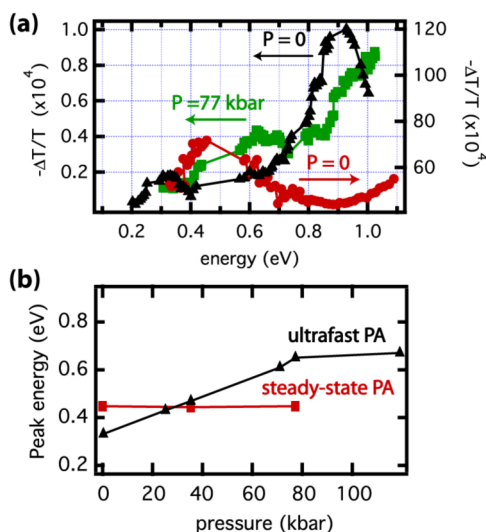


**Figure 1.** (a) Transient absorption spectra of a MEH-PPV film obtained in a diamond anvil cell. The left axis plots the subpicosecond PA, while the right axis is the steady-state PA (millisecond time scale). Black triangles show the ultrafast PA at ambient pressure (applied pressure = 0), and green squares show the ultrafast PA under 77 kBar. The red circles show steady-state PA at ambient pressure. (b) PA peak positions as a function of pressure. Black triangles show the shift in the ultrafast PA peak originating near 0.35 eV, while the red squares show that for the steady-state PA peak originating near 0.4 eV. The difference in their pressure dependence demonstrates that these two peaks arise from separate species. Adapted with permission from ref 28. Copyright 2011 American Physical Society.

the yield of excimers depends sensitively on both the identity of the polymer (PPV vs PT) and its' processing history; that stronger interchain interaction leads to a higher excimer yield, up to 30% in regioregular P3HT and 10% in MEH-PPV.<sup>30</sup> Allowing for differences in the processing history of the respective samples,<sup>56</sup> and the manner in which the transient species absorption coefficient was inferred, these estimates are qualitatively consistent with those made by Rothberg of a high yield of interchain species in PPVs.<sup>49,53,55</sup>

Moreover, although the excimer state appears to be predominantly dark, excimer emission has been observed in a number of conjugated polymers,<sup>54</sup> including MEH-PPV,<sup>55,57</sup> and LPPP.<sup>58</sup> This broadened emission, significantly red-shifted from the primary PL band, indicates that the excimer lies lower in energy than the intrachain singlet by several hundred millielectronvolts, as expected from its mixed resonance-stabilized configuration,<sup>27,54</sup> and as predicted by high-order configuration-interaction calculations on model PPV oligomers.<sup>28</sup>

Another compelling study that suggests the dominance of excimers comes from the work of Benjamin Schwartz. Schwartz has been prominent in advocating a nuanced view of excited-state dynamics in conjugated polymers, showing that the whole variety of interchain species discussed above, excimers, exciplexes, and polaron pair states, are likely present in MEH-PPV films depending on the excitation density and processing conditions.<sup>39,59</sup> Of particular note to the present discussion, Schaller and Schwartz used near field scanning optical microscopy experiments to determine which types of interchain species were present in MEH-PPV films and to spatially resolve their distribution.<sup>57</sup> These elegant experiments exploited the difference in solvatochromic shifts expected for emission from

interchain species with strong dipole moments such as exciplexes and polaron pairs, compared with that expected for interchain species with a weaker dipole, such as excimers. Schaller suggested that exposure to a polar solvent would red-shift emission from polaron pairs as the highly polarized excited state would be stabilized by solvation more than the ground state, narrowing the energy gap. Conversely, they suggested that emission from an excimer would be unchanged, or blue-shifted, upon immersion in a polar solvent since these authors expected the excimer to have a vanishing dipole while the ground state possesses a modest one.<sup>57</sup>

Figure 2 shows the near field PL spectra of annealed MEH-PPV films measured by Schaller et al., whose emission is

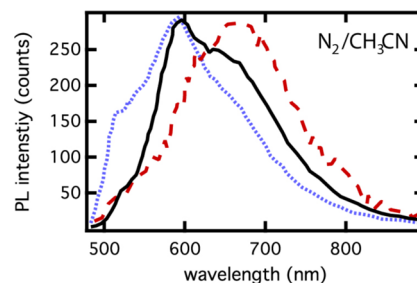


**Figure 2.** Near-field photoluminescence spectra obtained on an annealed MEH-PPV film. The black solid trace indicates the PL obtained under nitrogen atmosphere, while the colored dotted traces show the PL spectra obtained under liquid acetonitrile. The majority of the film (>95%) showed spectra similar to the dotted blue trace, while a few localized regions (<5%) showed spectra similar to the red dashed trace. Adapted with permission from ref 57. Copyright 2002 American Chemical Society.

thought to be predominantly from interchain species.<sup>56</sup> Upon introduction of a highly polar solvent (acetonitrile or ethylene glycol) the majority of the surface exhibited blue-shifted emission (blue dotted trace, Figure 2), which these authors interpret as indicating the dominance of nonpolar excimers. However, in a few locations, associated with no observable topographic feature, the emission was red-shifted (red dashed trace, Figure 2), indicating areas where exciplex or polaron pair formation was favored. These authors speculated that the localized regions of red-shifted emission, associated with polaron pairs or exciplexes, were caused by phase segregation of defects in the polymer chains, possibly including chain ends, carbonyl defects, or cis linkages. Moreover, they showed a tantalizing connection to the molecular weight of the polymer: lower molecular weight MEH-PPV exhibited more areas that produced polaron pairs. Nevertheless, in all cases the excimer dominated.

More recently, experimental techniques have emerged, such as two-dimensional electronic spectroscopy (2D ES), that present an alternative path toward identifying ultrafast transient species and determining their intra- or interchain nature. Recent work by some of the authors highlights the potential of this technique to help address this problem.

The key advantage of 2D spectroscopy is its capacity to increase the information content available from pump-probe experiments while maintaining the superior temporal resolution afforded by transform-limited laser pulses.<sup>60</sup> Several studies have revealed key insights into the nature of excited states and energy transfer processes in conjugated polymers.<sup>61–64</sup> A full description of the experimental technique is beyond the scope

of the present manuscript, and the interested reader is referred to several recent review articles as well as texts dedicated to the subject.<sup>65–71</sup>

As has already been pointed out, the continuum of neutral/charged states and overlapping resonances can make it difficult to assign spectral features to particular species. Another notable example is the  $\sim 660$  nm, subgap transient PA feature observed in neat P3HT that has been attributed to overlapping SE and electroabsorption due to charges<sup>33,35,72</sup> as well as a resonant photoinduced absorption from polymer polarons.<sup>73–75</sup>

We have carried out 2D ES experiments on neat RR-P3HT films in an attempt to provide further insight into the origin of this spectral feature. In the 2D experiments, two positive-going peaks along the diagonal are present at wavelengths corresponding to the 0–0 and 0–1 vibronic features in the linear spectrum (Figure 3). As the transitions responsible for

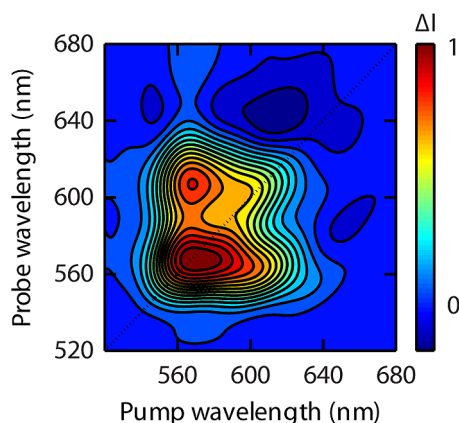


**Figure 3.** Real part of the total 2D electronic spectrum of 50 kDa P3HT film obtained at a waiting time of  $\sim 200$  fs.

these spectral features arise from the same ground state, cross peaks appear above and below the diagonal. In addition, we observe the subpicosecond rise of a negative-going, off-diagonal feature with excitation at  $\sim 600$  nm and detection at  $\sim 650$  nm. The formation of the excited-state absorption feature can be attributed to relaxation of the initially photogenerated exciton to form either a polaron or excimer species.

In the 2D data, the excited-state absorption feature is sufficiently spectrally resolved such that a full characterization of its temporal decay is possible. Overlapping stimulated emission is resolved, as well. A complete lifetime analysis of the 2D map may provide insight into the nature of the species responsible for this spectral feature akin to previous studies exploiting differences in the radiative lifetimes expected for intra- and interchain species.<sup>76</sup> Although at present this detailed kinetic analysis is not possible due to technical constraints, we anticipate continuing<sup>77–79</sup> and future developments to make this possible and extend the capabilities of the technique further.

Combined, the observations highlighted here and in the preceding section point to the importance of excimers, and interchain species in general, in the photophysics of conjugated polymers, if the results can be generalized from the test case of MEH-PPV. Perhaps more compelling than any individual experiment is the remarkable explanatory power of the hypothesis. Rapid formation of interchain species can explain the concentration quenching behavior of conjugated polymers<sup>55</sup> and the dependence of PL quenching on interchain

order observed, for example, in the case of regioregular and regiorandom P3HT.<sup>80,81</sup> It can also explain the long-lived tail often observed in the PL dynamics of conjugated polymers, as the exciton is reformed by thermal activation from the excimer state.<sup>55,82</sup> The prevalence of interchain excitations may have important consequences for operation of optoelectronic devices, as we will discuss in the concluding section.

## FORMATION OF FREE CHARGES

We have emphasized that charges are not produced *directly* by optical gap excitation of conjugated polymers except via second-order processes, artifacts of high pump fluence transient experiments. Nevertheless, charges are produced in conjugated polymers secondary to the initial photoexcitation, even in conditions of low pump fluence and little excess energy.<sup>10–15,83</sup> These charges persist into the nanosecond time scale and have been variously detected through conductivity,<sup>12,83</sup> transient absorption,<sup>13,34,36</sup> and delayed PL dynamics (Stark shift).<sup>84</sup> Interesting questions therefore arise: are charges produced from hot or thermalized excitons? Does excess excitation energy matter? What is the role of excimers? What is the effect of impurities and defects? What is the role of polymer microstructure? The remainder of this paper is dedicated to exploring these issues.

Several experiments indicate that free charges originate primarily from luminescent intrachain excitons, rather than evolving from the dark excimer state or other interchain species. The earliest clear example of this is a paper by Rothberg<sup>85</sup> using a “pump–dump” experiment on MEH-PPV, wherein the exciton population is dumped via stimulated emission at a varying delay after the initial excitation pulse while the integrated change in PL and photocurrent (PC) are measured. They found that dumping the exciton population through stimulated emission caused a correlated drop in both PL and PC. This lasted for a few tens of picoseconds before the PC became unaffected, while the PL continued to decay. This result suggests two conclusions: first that the species responsible for stimulated emission and PL (the intrachain exciton) is the source of free charge (photocurrent); second that exciton dissociation may only be efficient within the first few tens of picoseconds, prior to complete exciton relaxation within the inhomogeneously broadened density of states.

Nearly identical, and more complete, pump–dump experiments were later carried out by Müller and co-workers on LPPP, where the only difference in result was that photocurrent depletion due to dumping the exciton population extended throughout the exciton lifetime.<sup>52</sup>

These results are summarized in Figure 4a–c. Figure 4a shows the differential transmission dynamics at 2.49 eV, demonstrating stimulated emission with a single-exponential exciton lifetime of 180 ps. Figure 4b shows the concomitant change in integrated PL intensity with dump delay. The PL depletion dynamics match those for SE. Figure 4c shows that photocurrent through the film is also depleted by the dump pulse, and while photocurrent depletion decays twice as fast as PL depletion, at  $t = 0$  after photoexcitation the two match nearly quantitatively. On the basis of the correlation between relative change in PC and PL (both  $\sim 2\%$  at  $t = 0$ ), Müller and co-workers concluded that luminescent intrachain excitons were the *only* important source of free carriers. However, these authors also inferred a significant population of an interchain species from other experiments (5–25% total yield), which do not spontaneously dissociate to form free charge. An optical

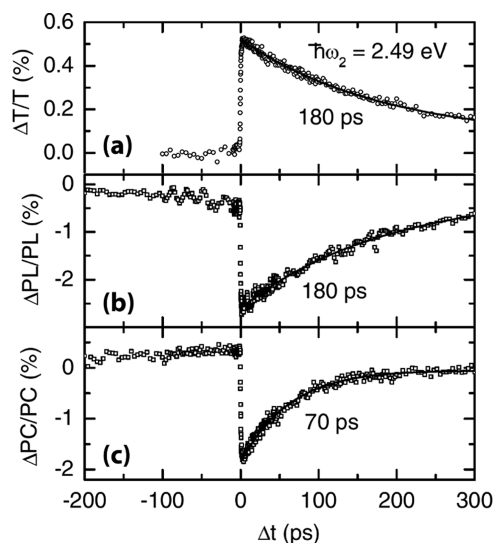


**Figure 4.** Differential changes in (a) probe transmission, (b) photoluminescence, and (c) photocurrent as a function of delay time between the pump and “dump” pulses on a film of ladder-type poly(*p*-phenylene) (MeLPPP). Reprinted with permission from ref 52. Copyright 2002 American Physical Society.

push pulse at an energy lower than that required for stimulated emission (1.9 vs 2.5 eV) was capable of efficiently dissociating this species and enhancing the measured photocurrent. A similar observation of push–pulse dependent photocurrent generation for donor–acceptor blends has recently garnered much attention.<sup>86</sup>

Additional evidence showing that charges evolve primarily from intrachain excitons comes from studies utilizing the field dependence of both transient absorption and PL dynamics in PPVs,<sup>44</sup> LPPPs,<sup>34,87,88</sup> and PT.<sup>13</sup> Most authors find that in PPVs and LPPPs exciton dissociation can extend throughout the exciton lifetime but that the efficiency of charge separation decreases with time,<sup>34,44,87,88</sup> while for polythiophene derivatives exciton dissociation into free charges continues unabated throughout the exciton lifetime.<sup>13,84</sup>

Those polymers (PPVs and LPPPs) that show a time-dependence of the apparent exciton dissociation rate constant also tend to show significant excitation energy dependence of carrier yield<sup>34,88</sup> and threshold type electric field dependence of carrier yield; those exhibiting little or no time-dependence (PTs) show only weak dependence of yield on initial excitation energy and no significant electric field threshold for charge separation.<sup>13,83</sup>

The transient absorption experiments cited here were carried out under the supervision of Villy Sundström,<sup>13,34,88,89</sup> and there is a key difference between them and most that are reported by others: the Sundström group has used the electric-field response of the transient absorption signal to identify the optical band used to probe charge carrier dynamics and to sort out other contributing spectral features, increasing confidence in the spectral and dynamical assignments.

Figure 5a and b shows the key result from the work of Zaushtsyn and Sundström. Figure 5a shows the PA dynamics obtained at 1.55 (circles) and 1 eV (triangles) probe energies on a poly(3-(4-octyl-phenyl)-2,2)-bithiophene (PTOPT) film. The signal at 1.55 eV was assigned to a combination of polaron and exciton absorption, while that at 1.0 eV was assigned purely to exciton absorption. Figure 5b shows the electric-field

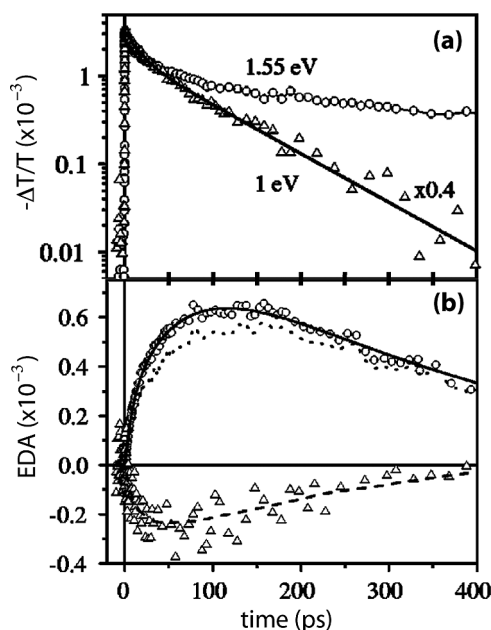


**Figure 5.** (a) Photoinduced absorption (PA) dynamics probed at 1.55 (circles) and 1 eV (triangles) on a film of poly(3-(4-octyl-phenyl)-2,2)-bithiophene (PTOPT). (b) Electric-field induced differential absorption (EDA) probed at 1.55 (dots) and 1 eV (triangles) on the same film. The PA signal at 1.55 eV contains a combination of contributions from excitons and charges, while that at 1.0 eV was assigned to pure exciton dynamics. The EDA signal at 1.55 eV was corrected for a small contribution from exciton depletion to calculate the pure charge dynamics in (b) (circles). Reprinted with permission from ref 13. Copyright 2004 American Physical Society.

modulated differential absorption (EDA) dynamics, where a pulsed electric-field was applied to the sample in order to separate out the polaron absorption signal from all other contributions. The polaron absorption, after a small correction for exciton depletion, is shown in the circular markers in Figure 5b. Strikingly, the polaron concentration begins at zero, and grows in over the course of 100 ps, similar to the observed exciton lifetime. We note that, while exciton–exciton annihilation might produce similar charge generation dynamics to those in Figure 5b, Zaushtsyn has ruled out this possibility by showing that increasing the pump fluence *decreases* charge yield.<sup>13</sup>

The results discussed in the last three sections paint a cohesive picture of charge separation in conjugated polymers, though it may not seem so at first glance. In all cases the primary photoexcitation appears to be a mixture of intrachain excitons and bound interchain species, likely dominated by excimers, with free charges evolving only from intrachain excitons. Polymers fall into two classes: those that require significant excess energy for efficient charge separation,<sup>34,44,88</sup> and those that do not.<sup>13,83</sup> However, this is not to suggest that polythiophenes, which require no excess energy for charge separation,<sup>13</sup> have a small exciton binding energy or that there is a dominant interband transition. For example, it should be kept in mind that the absolute yield of free carriers is generally 10% or less in these polymers,<sup>12–14,52</sup> and, as demonstrated in Figure 5b, that charge generation and exciton dissociation take place over tens to hundreds of picoseconds. Rather, the barrierless charge generation process in PTs indicates a limited concentration of exciton dissociation sites within the polymer, producing exciton diffusion and site-concentration limited



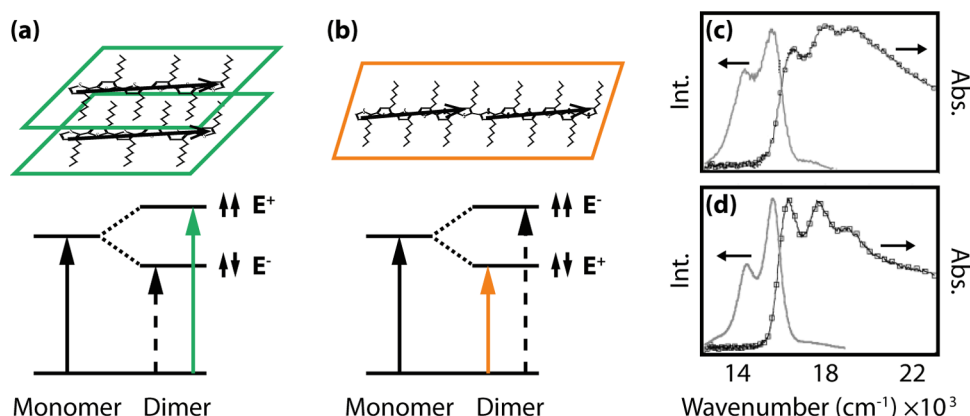


**Figure 6.** Pictorial representation of (a) H- and (b) J-aggregates in P3HT. Coupling between  $\pi$ -stacked polymer chains through-space leads to H-aggregation, while coupling between chromophores along the polymer backbone results in J-aggregation. In the simplest case of a dimer, two configurations are possible in each case. For the H-aggregate, the lowest energy configuration is in the form of antiparallel dipole vectors; in the higher energy case, the dipole vectors are oriented parallel. Only the latter is capable of coupling with the incoming light electric field, while the former is a forbidden transition. For J-aggregates, parallel head-to-tail dipole moment vectors are the lowest energy and are capable of coupling to the incoming light electric field. The highest energy transition is manifest in the opposite orientation of dipole moment vectors and is incapable of coupling to the incoming light electric field. Experimental absorption and PL spectra of P3HT nanofibers assembled and dispersed in solutions of (c) anisole and (d) toluene. The relative intensities of the vibronic peaks in c are indicative of H-aggregates, while those in d are indicative of J-aggregates. Adapted with permission from ref 102. Copyright 2013 American Chemical Society.

charge separation.<sup>89</sup> Indeed, a theoretical model has been proposed that explains charge generation in terms of structural defects in the polymer, be they physical, such as chain ends or torsions, or chemical, such as carbonyl defects that break conjugation.<sup>90</sup>

As with the supposition that the formation of excimers is a ubiquitous feature of conjugated polymer photophysics, the assertion that charges evolve primarily from breakup of luminescent intrachain excitons has impressive explanatory power. Several authors, including ourselves, have used kinetic models that invoke exciton-charge quenching to explain the decrease in apparent charge photogeneration yield in conjugated polymers with increasing excitation fluence.<sup>10,12,31</sup> Such behavior cannot be adequately accounted for by exciton-exciton quenching.<sup>10</sup> In one case we have used an exciton-charge quenching model to extract important physical characteristics of the polymers, such as doping density and the absorption coefficient of the positive polymer polaron, which are corroborated by independent techniques.<sup>12</sup> Analysis of these data rely wholly on the assumption that charges evolve from excitons and are not produced either directly or through interchain species that were produced on an ultrafast time scale. Any model of conjugated polymer photophysics that invokes ultrafast formation of free charge will have to provide an alternative explanation for these results.

Despite the intense study of conjugated polymer photophysics highlighted so far in this perspective, the question of how charges are created from a bound exciton in neat conjugated polymers remains unanswered. However, there are important hints. The study noted above,<sup>90</sup> suggesting that sharp torsions or other breaks in conjugation can form exciton dissociation sites, coupled with the spatial heterogeneity in the type of interchain species observed by Schaller in MEH-PPV,<sup>57</sup> leads to the interesting possibility that it is the crystalline microstructure of the polymer that controls charge separation—the microstructure of PT derivatives is markedly different from either PPV or PPP, showing, for example, much greater crystallinity. This correlates nicely with the sharp difference in

the photophysics of PT relative to that of PPV and LPPP as already discussed.<sup>89</sup>

Numerous authors have suggested a connection between the microstructure of conjugated polymers and their photophysics,<sup>11,30,53,56,57,73,80,91,92</sup> even providing qualitative correlations.<sup>11,30,56,92</sup> It is clear from these studies that both the yield of excimers and free charges is related to the degree of interchain interaction that takes place in the film. Indeed, this qualitative observation has been used to enhance the luminescence efficiency of PPV derivatives by adding bulky side chains<sup>93</sup> or diluting the active material in an inert host<sup>53,94,95</sup> to limit polymer chain aggregation. Nevertheless, no specific hypothesis has been put forward describing how the microstructure of a conjugated polymer controls its photophysics. In the following sections, we discuss what is known about polymer microstructure, how it is connected to the photophysics of films, and ultimately how it controls charge generation in polythiophene derivatives.

## ■ AGGREGATES AND THE ABSORPTION SPECTRUM

The molecular packing of conjugated polymers is often investigated through the effects that intermolecular interactions have on their absorption and emission spectra. Owing to a significant frequency change of a torsional mode between the ground and excited electronic state, the absorption spectrum is broad, while the fluorescence is more structured (see ref 96 and references therein). For this reason, the structured, red-shifted photoluminescence spectrum has proven more informative.

Several models have been employed to extract microscopic information from changes in absorption and emission spectra, typically as a function of temperature or solvent. Collison et al., for example, observed a drastic change in the photoluminescence spectrum of MEH-PPV as a function of solvent composition.<sup>97</sup> They found two distinct fluorescence spectra for MEH-PPV dissolved in a “good” solvent and a “bad” solvent. The spectrum observed for the 60:40 ratio of “good” to “bad” solvent could be reproduced with a superposition of the two pure-solvent spectra. These findings were interpreted in terms of a two species model including isolated and aggregated PPV



polymer chains called the blue and red species, respectively.<sup>97</sup> These entities exhibit nearly identical spectral profiles, with the red-shift of the red-emitting species attributed to planarization of the polymer backbone induced upon aggregation. These species have also been identified in single molecule spectroscopy experiments and connected to distinct polymer conformations.<sup>98</sup> Köhler et al. found it possible to observe these species in MEH-PPV in the same solvent as a function of temperature.<sup>99</sup> They employed an expanded Franck–Condon deconvolution analysis to simulate the absorption and photoluminescence spectra of MEH-PPV within the two-species model.<sup>99</sup>

More subtle effects than spectral shifts are also manifest upon aggregation. Even in the absence of excimers, in cases where the electronic coupling is not so strong and does not involve interchromophore orbital overlap, chromophore aggregates can perturb spectra according to the Frenkel exciton model. The effects of aggregation on the optical absorption spectrum of molecular aggregates were established early on by the work of Kasha and Hochstrasser, among others.<sup>100,101</sup> Two limiting cases are most helpful to illustrate this picture: one in which the molecules are stacked head-to-tail (J-aggregate) and the other in which the molecules stack in a sandwich configuration (H-aggregate). In the case of J-aggregation (Figure 6b), optical coupling between the ground-state and the lowest excited-state in the exciton manifold is permitted, while coupling to the highest state is forbidden. For H-aggregates (Figure 6b), the opposite holds true. A useful feature of the model is that it gives insight into molecular packing via readily observable shifts in transition intensities in the optical spectra. See, for example, Figure 6c and d.<sup>102</sup>

In the case of conjugated polymers, typically either H- or J-character is observed. The classic example of J-aggregation is polydiacetylene,<sup>103</sup> while P3HT is an example in which the optical absorption spectrum exhibits contributions from H-like aggregates and unaggregated species.<sup>104</sup> Gray and co-workers recently demonstrated that P3HT nanofibers in solution could exhibit J-like character and that the H- or J-like character could be tuned by changing the temperature, pressure, or solvent (see Figure 6c and d).<sup>102,105</sup>

Spano and co-workers have employed a perturbative polaron treatment (exciton-polaron) to predict and analyze optical lineshapes in molecular crystals, polyacenes, and conjugated polymers.<sup>18,106,107</sup> In addition to calculating the electronic properties of aggregates in the very strong electronic coupling limit, where vibrations can be ignored to a good approximation,<sup>108</sup> the polaron model can calculate spectra in other limits, within certain constraints that we will not discuss here. Spano and co-workers have shown the remarkable power of this theory for elucidating the percentage of H-character and delocalization length from optical spectra parameters such as the free exciton bandwidth. The model has been particularly apt at describing the temperature-, pressure-, and solvent- induced changes observed in P3HT nanofibers,<sup>102,105</sup> films, and solutions.<sup>104</sup>

Cornil and co-workers have carried out a number of quantum-chemical studies investigating the effect of interchain interactions on the optical properties and nature of excited-states in conjugated oligomers and polymers.<sup>109–114</sup> Three features of their work stand out in the present context: (1) the experimental absorption spectrum can be reproduced for phenylenevinylene oligomers,<sup>109</sup> (2) the calculations reproduce the qualitative features predicted by the exciton model

described above,<sup>110,111</sup> and (3) the supermolecular approach<sup>113</sup> provides additional information on the nature of the intrachain and interchain excited-states by expanding upon the traditional exciton model and including charge-transfer character.<sup>112</sup> For example, the lowest-energy state for DMOS-PPV/CN-PPV was predicted to be intrachain, while the lowest-energy state for MEH-PPV/CN-PPV was predicted to be interchain and exhibit charge-transfer character.<sup>114</sup> These findings provided a foundation upon which to interpret the experimental results that charge transfer occurs in MEH-PPV/CN-PPV whereas energy transfer occurs in DMOS-PPV/CN-PPV.<sup>112</sup>

As we have just briefly reviewed, several microscopic models have been developed to describe the optical spectra of conjugated polymers and have provided a more detailed understanding of the connections between molecular packing, electronic properties, and the nature and prevalence of interchain species in conjugated polymers. While these microscopic models have provided exceptional insight into molecular-scale structural and electronic properties, it is still unclear what role these microscopic properties play in charge separation in neat conjugated polymers. A discussion of long-range structural order follows.

## ■ POLYMER MICROSTRUCTURE

Until quite recently, work on conjugated polymer photophysics had proceeded under the assumption that conjugated polymers do not adopt an understandable long-range structural motif. Nevertheless, a wealth of information is available from studies of saturated polymers that can inform our discussion of their conjugated cousins. Largely due to the work of Natalie Stingelin,<sup>14,15,115–120</sup> Martin Brinkmann,<sup>121–123</sup> and others,<sup>124–126</sup> awareness of this rich historical knowledge base is growing within the community.

As the length of a linear molecule is increased from the regime of small molecules, to oligomers, to that of high polymers, two important changes occur in their self-organization that lead to dramatic changes in bulk properties: the onset of chain folding and that of entanglement. Entanglement and its consequences are easily envisioned; a collection of very long disordered molecules will tend to wrap around one another, conferring cohesion and elasticity to the bulk material not observed in crystalline or amorphous ensembles of small molecules. It is this characteristic of intermolecular load transfer that confers the physical characteristics we associate with plastics: tensile strength, elasticity, and plastic deformation. In the case of conjugated polymers, entanglement appears to be crucial for efficient bulk charge transport.<sup>119,127–130</sup>

Chain folding, an important feature of high polymer crystallization, is a subtler general property of large linear molecules and is likely to occur at somewhat lower molecular weights than the onset of entanglement.<sup>131</sup>

Keller provided an excellent tutorial-review on the subject of polymer crystallization in 1968,<sup>132</sup> an updated view was presented by Ungar in 2001,<sup>133</sup> and text books are available on the subject.<sup>134</sup> Despite the well-established nature of this subject, we feel that there is value in summarizing the salient features here, as much of the audience at which this paper is aimed will not have been formally trained in materials science. The interested reader is encouraged to obtain the original sources for greater detail.

The case for chain folding is this. Early X-ray diffraction (XRD) observations of bulk polymer samples had long shown

moderate crystallinity, but it was not until the 1950s that advances in synthetic methods allowed the preparation of highly crystalline samples. For the first time, single crystals of polymers were grown from solution and characterized by XRD and scanning electron microscopy (SEM). These studies presented a curious picture: polyethylene formed lamellar (platelike) crystals with a thickness of ca. 10 nm, where the polymer backbone was oriented within the crystal thickness, orthogonal to the much larger dimensions of the crystal. Yet the molecular weight of the polymer implied a chain length much, much longer than the crystal thickness. The conclusion was that the polymer chain must fold back on itself, forming ribbons of folded chains that subsequently stack into lamellae.<sup>132</sup> Indeed, Keller later proved that given the steric freedom to do so, these folds take the form of sharp adjacently re-entrant hairpins.<sup>131</sup> However, in the complicated, sterically hindered context of high concentration, high molecular weight polymers, the exact nature of the lamellar surface—how ordered and the prevalence of adjacently re-entrant chains—is still a matter of debate.<sup>133</sup> Figure 7a shows a cartoon of a perfect lamellar crystal with adjacently reentrant folds. Only a monodisperse sample crystallized from dilute solution would approach such perfection.<sup>131</sup>

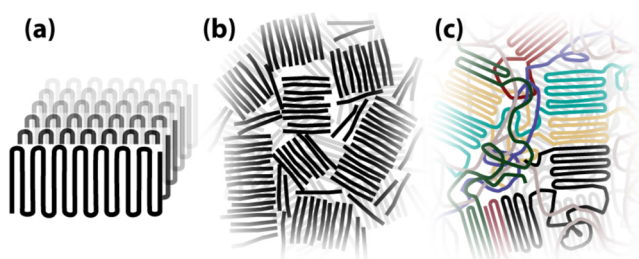


**Figure 7.** Cartoons of different polymer (and oligomer) microstructures. (a) Perfect folded chain crystal. (b) Paraffinic structure adopted by oligomers; characterized by extended-chain crystals. (c) Semicrystalline microstructure adopted by many high molecular weight polymers; composed of lamellar aggregates embedded in an amorphous matrix and characterized by extensive chain entanglement and folding.

This folding behavior is intrinsic to flexible linear molecules and is controlled by a kinetic mechanism. At any given time there is a finite probability that the extended polymer chain in a solution or molten phase will fold back on itself through random thermal motion. The fold only “sticks” if the fold length is long enough that the enthalpy decrease associated with self-crystallization outweighs the obvious entropic penalty, the increase in surface energy of the incipient crystal, and the energetic cost of bending the polymer backbone. Since random initiation of smaller fold lengths are, in general, more probable than long ones, the crystal will continue to grow at the minimum thermodynamically stable fold length (lamellar thickness) for a given temperature and solvent.

Control of the fold length through solvent identity and crystallization temperature was demonstrated to be a universal feature of polymer crystallization. It is the degree of supercooling, i.e. the difference between the dissolution temperature and the crystallization temperature, that determines the fold length rather than the absolute crystallization temperature, leading to an obvious dependence on solvent quality. Smaller supercooling (higher crystallization temperature in a given solvent) leads to a longer fold length as this parameter

modulates both the entropy loss term associated with crystallization and the decrease of enthalpy relative to the solvated chain.

The complete picture that emerges for any given polymer chain length depends on the interplay of chain folding and entanglement. For oligomeric materials with chain lengths below the entanglement limit a “paraffinic” structure forms, characterized by chain extended crystals, likely also accompanied by unhindered chain folding depending on the molecular weight and crystallization conditions (figure 7b). For polymeric materials above the entanglement limit, a “semicrystalline” structure forms, characterized by folded chain lamellar stacks embedded in an amorphous matrix formed from chain ends, loops, and loose cilia which decorate the lamellae surfaces (Figure 7c). Though, as noted above, the extent to which reentrant folds exists in the context of high concentration, high molecular weight samples is not known. A prominent feature of the semicrystalline structure is that individual polymer chains will often contain both amorphous and crystalline segments that may extend across multiple crystalline and amorphous domains. These interconnecting molecules are known as tie-chains.

The reader may justifiably question whether these results describing the microstructure of flexible polymers are really applicable to the behavior of conjugated polymers, which are thought to be significantly more rigid, particularly given the important role of sharply re-entrant folds in the apparent structure of flexible polymers. Nevertheless, evidence is accumulating that, at least for polythiophene derivatives, the structural understanding developed for saturated polymers may be applied to conjugated polymers without significant modification.

Take for example the now ubiquitous growth of nanofibers from soluble polythiophene derivatives.<sup>105,124,125,135–137</sup> Liu and co-workers showed qualitatively that these supermolecular assemblies follow the same scaling laws laid out for single crystals of saturated polymers.<sup>124</sup> For low molecular weight P3HT the nanofiber width (equivalent to the lamellar thickness discussed above) scaled with molecular weight. However, once the chain length reached a certain threshold ( $\sim 14$  nm in this case), the nanofiber width saturated, indicating the onset of chain folding. Likewise, for high molecular weight P3HT, it was possible to tune the nanofiber width by varying the crystallization temperature, just as previously described for saturated polymers.<sup>132</sup>

These effects are not limited to the formation of nanofibers in dilute solution. Brinkmann has shown a similar correlation between the molecular weight of P3HT and the lamellar thickness in bulk samples.<sup>121,122</sup> Once the molecular weight of P3HT rose above  $\sim 10$  kg/mol, the lamellar thickness saturated at  $\sim 2.5$  nm.

In addition to these powerful inferences, re-entrant folds have been directly observed for a variety of poly-(alkylthiophene) derivatives via scanning tunneling microscopy.<sup>138–141</sup> While the polymer structure in these cases is likely strongly influenced by the graphite substrates on which the samples were prepared, we find the direct observation that even conjugated polymers spontaneously form sharp adjacently re-entrant folds quite suggestive.

On the basis of these results we suggest that the classical polymer science description of polymer microstructure is generally applicable to conjugated polymers and that chain-folded crystals will be present in high molecular weight

polymers where crystallization occurs. How rigid a polymer backbone must become before chain folding ceases is an interesting question that merits future research, which may profoundly affect the optoelectronic characteristics of such highly rigid polymers relative to their more flexible cousins. Recent work on some low optical gap copolymers suggests that the large repeat unit in these systems makes them substantially more rigid than P3HT,<sup>142</sup> which may inhibit or preclude chain folding.

## CORRELATING MICROSTRUCTURE AND CHARGE PHOTOGENERATION

In recent work by some of the present authors, we have shown that the specific features of polymer crystallization discussed in the previous section have a strong influence on photoinduced charge carrier production in polythiophene derivatives. Specifically, that charge carrier yield is correlated with the aggregate surface area of the folded chain lamellar crystals.<sup>14,15</sup>

In these papers we use two primary methods to control the polymer microstructure: molecular weight and crystallization temperature. The discussion above has already outlined the predictable influence of these two parameters: molecular weight determines whether the polymer adopts a paraffinic or semicrystalline structure, while the crystallization temperature modulates the lamellar thickness in the semicrystalline regime.

Figure 8 shows the key findings of our work varying the molecular weight. The vertical axis displays the yield-mobility

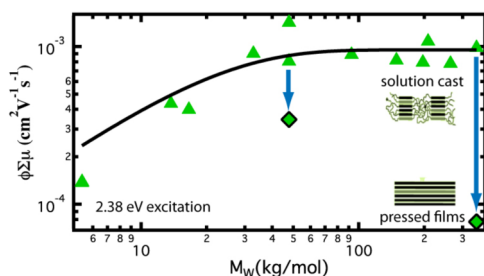


**Figure 8.** Product of charge photogeneration yield and gigahertz charge carrier mobility ( $\phi\Sigma\mu$ ) measured via time-resolved microwave conductivity on films of P3HT as a function of the polymers molecular weight. The green triangles are the results for solution cast films. The black-framed green diamonds are the results for films molded in the solid-state. Reprinted with permission from ref 14. Copyright 2012 Wiley-VCH.

product derived from time-resolved microwave conductivity (TRMC) experiments plotted as a function of molecular weight. We argued in the original paper<sup>14</sup> that the changes in yield-mobility product were dominated by changes in the yield, with little or no change in the GHz charge carrier mobility, and pulse radiolysis experiments have verified this contention.<sup>143</sup> The yield of free photogenerated charge increases by almost an order of magnitude as we move from P3HT samples with  $M_w = 5$  kg/mol to those above 30 kg/mol: as the sample transitions from one dominated by chain extended crystals to one composed of folded chain crystals embedded in an amorphous matrix.

The shape of this curve is strikingly similar to the saturation behavior observed for lamellar thickness, indicative of the transition from a paraffinic structure to a semicrystalline one and the onset of chain folding.<sup>121,122,124,133</sup> It is also quite similar in shape to trends derived for field-effect mobility as a

function of molecular weight,<sup>127,143</sup> which has been attributed to an increase in tie chain density that facilitates transport between crystalline domains.<sup>119</sup>

In order to demonstrate that this trend of increasing carrier yield is not simply a function of total crystallinity, we also employed a novel processing method: solid-state molding. This method has been demonstrated to dramatically increase the crystallinity and lamellar thickness of high molecular weight P3HT with a concomitant increase in time-of-flight hole mobility of close to 2 orders of magnitude.<sup>115</sup> However, when we measure the yield mobility product for such samples with TRMC (black-framed green diamonds, Figure 8), we find that it is an order of magnitude lower than that found for solution-cast samples of the same (350 kg/mol) molecular weight, which change we again argue is predominantly due to the yield. Finally, lest it be thought that P3HT is a unique case, we note that the same trend of increasing charge photogeneration yield in a neat polymer with increasing molecular weight has been observed for Si-PDTBT.<sup>129</sup>

In the original paper, we attributed the increase in charge photogeneration yield to the interface between amorphous and crystalline domains: low molecular weight samples with no strictly amorphous component have low yield, as do molded samples with their very high crystallinity. Similarly, regiorandom P3HT, which is predominantly amorphous, also exhibits low photogeneration yield.<sup>144</sup> Only in samples where the amorphous and crystalline phases coexist do we observe large photogeneration yield, approaching 10%.

However there is a second possibility that has yet to be explored: that sharp chain folds are the “defect” which facilitates charge photogeneration. This hypothesis is also consistent with the observed facts: samples with chain extended conformations, produced either through low molecular weights or solid-state molding, produce little photogenerated charge. Similarly, the amorphous regiorandom material is not expected to exhibit a high density of sharp bends as they are clearly not energetically favorable and will only be stabilized by concomitant chain crystallization. Only the semicrystalline samples with chain-folded crystals exhibit a large photogeneration yield. We will return to this idea later in the discussion.

We now turn to more recent work, where we use controlled crystallization temperatures to tune the lamellar thickness in two polythiophene derivatives: poly(2,2':5',2'':3,3'':dicyclopentylthiophene) (PTTT-10) and P3HT.<sup>15</sup> We have shown that the predictions of classical polymer science hold in both polymers: increased crystallization temperature results in both larger lamellar stacks and thicker crystalline lamellae. X-ray diffraction coherence lengths in the alkyl stacking direction double from 5 to 10 nm as the crystallization temperature is increased from 26 to  $\sim 100$  °C in PTTT-10. In addition, both the enthalpy of fusion and the melting temperature increase, as measured via differential scanning calorimetry. This demonstrates both enhanced crystallinity (enthalpy of fusion) and increased lamellar thickness (melting temperature).<sup>132</sup>

The TRMC results for charge photogeneration yield in these samples are consistent with our previous experiments varying the molecular weight. Increased lamellar thickness leads, in general, to a decrease in charge photogeneration yield for both PTTT and P3HT. This is as expected, since large crystals have both a lower surface area per crystal (interface with the amorphous phase) and a lower density of chain folds.



## ■ FORMATION OF CARRIERS IN NARROW GAP COPOLYMERS

While thus far we have discussed the generation of carriers in neat homopolymers, charge photogeneration in narrow gap copolymers has recently garnered substantial interest. Although narrow gap copolymers are nothing new,<sup>145,146</sup> the synthesis of high-molecular weight, processable copolymers including PCDTBT,<sup>147</sup> PBDTTPD,<sup>148</sup> and PTBs,<sup>149,150</sup> that exhibit record-breaking photovoltaic efficiencies<sup>151,152</sup> have rekindled interest. These materials have been excluded from the preceding discussion in large part because much less is known about their photophysics, and it is possible that the push–pull motif of alternating units with differing electron affinities could substantially alter the picture we have arrived at for homopolymers.

The donor–acceptor (or “push–pull”) moieties along the polymer backbone in narrow gap copolymers has called into question the nature of the transitions appearing in the optical absorption spectrum. Semiempirical quantum-chemical ZINDO calculations indicate charge-transfer character in the direct optical transitions of these materials.<sup>153</sup> While controversy exists over whether or not both optical absorption bands<sup>154</sup> or only the low-energy band exhibit charge-transfer character,<sup>153,155</sup> there is some consensus that the lowest-energy band exhibits partial charge-transfer character. The polarized nature of the excited state has been proposed to facilitate charge separation in bulk-heterojunction blends.<sup>156</sup>

Tautz et al.<sup>157</sup> recently assayed several narrow band gap copolymers for polarons applying the traditional assignment of the polaron feature in the mid-infrared. Reinterpreting this feature more generally as arising from interchain species, their data show a considerably enhanced yield of this species on the ultrafast time scale (relative to P3HT) in narrow gap copolymers. Furthermore, the distance between and electron affinity of subunits along the polymer backbone were varied, and it was found that while increasing the electron affinity of the acceptor subunit increased the overall yield of interchain species, this also resulted in a rapid, subsequent subpicosecond time scale decay. In contrast, increasing the distance between donor and acceptor subunits caused the interchain species yield to decrease. Thus, there was an optimal balance between the electron affinity of the acceptor subunit and distance between donor and acceptor subunit. In general, the interchain species yield assessed in this manner was much larger for the narrow gap copolymers than for P3HT.

Rolczynski et al. have suggested that separated charges are generated intramolecularly in narrow gap PTB-based copolymers.<sup>158,159</sup> They used near-infrared transient absorption spectroscopy to investigate a series of narrow gap copolymers with varying levels of fluorine substitution. The spectral features appearing in the near-IR TA spectrum were assigned to three different components: excitons, pseudocharge transfer states, and separated carriers. Global fits to their data indicated a substantial fraction of separated carriers appearing on the picosecond time scale and remaining on the nanosecond time scale. Calculations on monomers suggested a greater dipole moment change upon optical transition in several of the monomers of the narrow gap copolymers. These authors suggested a mechanism in which a more polarized exciton (i.e., larger dipole moment change) may have a high probability of forming separated carriers, whereas the less polarized exciton (i.e., smaller dipole moment change) would be more likely to

form the pseudo-charge transfer state. The authors also observed a linear correlation between the materials generating a higher fraction of separated carriers (in relation with the amount of pseudocharge transfer states) against the device power conversion efficiencies. The supposition that an exciton with more charge-transfer character in narrow gap copolymers may facilitate charge separation is supported by solvent-dependent steady-state absorption and photoluminescence and 2D ES experiments reported by Hwang et al. on two narrow gap conjugated polymers, PBDTTPD and PCDTBT.<sup>63</sup>

While the above-mentioned studies offer alternative explanations for the separation of carriers in narrow gap copolymers, the study of these materials is still rather incomplete. One idea, which fits with the apparent importance of excimers in homopolymers, is the possibility that neighboring donor and acceptor units (on adjacent chains, rather than along a chain) may form a classic exciplex after photoexcitation. Recent reports are highly suggestive of excited-states with significant charge-transfer character in these materials.<sup>160</sup> It may still be necessary to repeat some of the key experiments done on homopolymers, such as studying the pressure-dependence of the transient absorption spectra, in order to fully understand the photophysics of this new class of polymers. It is interesting to note that a recent TRMC study looking at one of the quintessential donor–acceptor polymers (PCDTBT) revealed a lower yield of photogenerated charge on the nanosecond time scale than did the control sample of P3HT,<sup>12</sup> coming in at just 0.7%.

## ■ SUMMARY, IMPLICATIONS, AND CONCLUSIONS

We have reviewed the evidence for charge separation in neat conjugated polymers, focusing on the heavily studied homopolymer backbones LPPP, PPV, and PT. We find that there is compelling evidence that the primary photoexcitations in these conjugated polymers are a combination of intrachain excitons and excimers/aggregates. Charges evolve from the emissive species associated with photoluminescence and stimulated emission (the exciton) over tens to hundreds of picoseconds. Previous reports of efficient subpicosecond photogeneration of free charge are explained by a combination of mistaken identity and second-order effects. In the first case, the excimer transient absorption spectrum is quite similar to that of the polaron, making accurate assignment of congested PA spectra extremely difficult. In the second, exciton–exciton annihilation and sequential excitation produce high-energy excited states with sufficient energy for direct charge separation and high initial charge transfer character.

Certain polymers such as PPVs and LPPPs appear to require either large applied electric fields or excess excitation energy in order for charge separation to proceed efficiently (~10%), while others, such as PT, do not.

These results are consistent with the view that free charge generation is mediated by a limited concentration of dissociation sites that are reached through exciton energy migration. The microstructure of neat semiconducting polymers can help us understand some of this behavior. A semicrystalline morphology with coexisting amorphous and crystalline domains appears to be a prerequisite for efficient charge separation, with the yield of free carriers in P3HT and PTTT-10 correlating with the surface area of the crystalline aggregates in the semicrystalline regime. This observation could explain the major differences in charge generation between PT



on the one hand, and PPVs and LPPPs on the other. PT is typically semicrystalline, while PPVs and LPPPs are not.

Despite these strong correlations between polymer microstructure and charge photogeneration yield, the fundamental mechanism of charge separation remains elusive.

Although we have focused almost exclusively on neat polymers in this review, it is important not to lose sight of the fact that the most compelling application of these materials is in low-cost solar cells. The picture of conjugated polymer photophysics that we present has some potentially interesting features from this perspective. In particular, the apparently ubiquitous ultrafast formation of interchain species that are lower in energy than the singlet exciton is intriguing. This is not a process that is often discussed in the organic photovoltaics literature. The typical description of OPV device operation begins with the assumption that light absorption results in an intrachain exciton whose energy can be readily estimated from the absorption edge. This hypothetical exciton subsequently undergoes migration via energy transfer, eventually reaching a heterojunction where charge separation can take place with near unit efficiency.

If a substantial fraction of excitations relax to form excimers on an ultrafast time scale as suggested here, this picture of charge generation in OPVs must be modified. First, since the excimer has no ground state absorption and the aggregate is only a weak one, it may not be possible to accurately estimate the energy of a significant fraction of the excited states present in the material. This will result in a systematic overestimation of Gibbs energy for the electron transfer reaction. Second, because of their low energy and low luminescence efficiency, excimers and aggregates will act as energy traps, immobilizing the exciton that would ideally have diffused to a donor/acceptor interface.

With these two effects in mind, we suggest that the prevalence of excimers and aggregates in conjugated polymers can help explain some otherwise puzzling features of OPV device operation. First, it is commonly observed that significant excess energy offset between the donor and acceptor molecular energy levels is required to drive charge separation with unit efficiency.<sup>161–168</sup> Yet charge separation can take place efficiently without excess energy when the charge-transfer state is pumped directly.<sup>169</sup> This apparent contradiction might be partly explained by systematic overestimation of the energy available from a significant fraction of extant excited states in the system. Second, it has recently been observed that (1) charge generation in polymer:fullerene blends may take place predominantly within the mixed phase rather than at an interface between pure materials<sup>170–173</sup> and (2) charge separation in P3HT:PCBM occurs not via electron transfer to the fullerene but by energy transfer to the fullerene and subsequent back hole transfer to the polymer.<sup>174</sup> Both of these observations are consistent with rather immobile excited states, requiring, on the one hand, very close proximity between intimately mixed fullerene and polymer in the amorphous phase and, on the other, the driving force of energy transfer from the polymer to the rather low-energy exciton of the fullerene in order to detract the excited state in the polymer. This picture of excimer rather than exciton splitting in OPV materials leads to the conclusion that a fullerene must be located within 2–4 nm of the initial excited state (a typical range for energy transfer in isotropic systems) in order for charge separation to occur, rather than the more commonly quoted 10–15 nm.

While speculative, these concluding remarks illustrate why it is crucial that we understand the fundamental photophysics of conjugated polymers—a goal that we remain far short of. There are still many things we do not understand about these materials. What is the mechanism of charge generation in neat films? Are chain folds important? How do excimers and related interchain species affect the operation of organic photovoltaic devices? Are donor–acceptor polymers mostly similar to, or very different from, homopolymers in their photophysics and charge generation mechanism? It is our hope that this perspective will help to stimulate new interest and experiments in this fundamental and fundamentally important field.

## AUTHOR INFORMATION

### Corresponding Author

\*E-mail: garry.rumbles@nrel.gov.

### Notes

The authors declare no competing financial interest.

### Biographies

Dr. Obadiah Reid received his B.S. in chemistry from Pacific University in 2004. He earned his Ph.D. in chemistry from the University of Washington in 2010. At present he is perusing postdoctoral research at the National Renewable Energy Laboratory. His interests are in studying charge generation, transport, and recombination processes in organic semiconductors.

Dr. Ryan Pensack received his B.A. in chemistry from Rutgers–Newark University in 2006. He earned his Ph.D. in chemistry from Penn State University in 2012. He is presently working in the research group of Gregory Scholes at the University of Toronto as a postdoctoral fellow. His primary research interests include developing ultrafast and multidimensional optical spectroscopy techniques to investigate electronic processes in organic photovoltaic materials.

Yin Song received his B.S. degree in Chemistry from Peking University in 2009. He is currently a Ph.D. candidate in Scholes group at University of Toronto. His research interests mainly focus on studying energy-transfer and charge-transfer dynamics in organic semiconducting materials by using ultrafast spectroscopic techniques.

Greg Scholes is the D.J. LeRoy Distinguished Professor at the University of Toronto in the Department of Chemistry. His research group examines photophysics in systems ranging from semiconductor nanocrystals to conjugated polymers to photosynthetic light-harvesting proteins. He is especially interested in uncovering microscopic details of light-induced energy capture and conversion processes in photosynthesis and organic photovoltaics using a combination of femtosecond laser experiments and theory. Dr. Scholes serves as an Editorial Advisor for *New Journal of Physics* and Senior Editor for the *Journal of Physical Chemistry Letters*.

Dr. Garry Rumbles is a Research Fellow at the National Renewable Energy Laboratory and Professor Adjoint in the Department of Chemistry and Biochemistry at CU Boulder. Dr. Rumbles joined NREL in 2000 and is widely recognized for his research in photochemistry and photophysics of conjugated molecular systems, energy conversion in organic light emitting diodes and organic photovoltaic devices, and nanoscale morphology.

## ACKNOWLEDGMENTS

G.D.S. thanks the National Science and Engineering Research Council of Canada for financial support. This work was supported by the Laboratory Directed Research and Development (LDRD) Program at the National Renewable Energy

Laboratory under task number 06RF1201 and the U.S. Department of Energy under Contract No. DE-AC36-08-GO28308 with the National Renewable Energy Laboratory. O.G.R. and G.R. thank Natalie Stingelin for many edifying discussions on the subject of polymer microstructure.

## ■ ABBREVIATIONS

PL, photoluminescence; PC, photoconductivity; SE, stimulated emission; PA, photoinduced absorption; TA, transient absorption; PPV, poly(*p*-phenylene vinylene); PT, polythiophene; LPPP, ladder-type poly(*p*-phenylene); PCDTBT poly-[*N*-9'-heptadecan-2,7-carbazole-*alt*-5,5-(4',7'-di-2-thienyl-2',1',3'-benzothiadiazole)]

## ■ REFERENCES

- (1) Moses, D.; Wang, J.; Yu, G.; Heeger, A. J. *Phys. Rev. Lett.* **1998**, *80*, 2685–2688.
- (2) Moses, D.; Dogariu, A.; Heeger, A. J. *Phys. Rev. B* **2000**, *61*, 9373.
- (3) Moses, D.; Dogariu, A.; Heeger, A. J. *Chem. Phys. Lett.* **2000**, *316*, 356–360.
- (4) Yu, G.; Phillips, S.; Tomozawa, H.; Heeger, A. J. *Phys. Rev. B* **1990**, *42*, 3004–3010.
- (5) Yoshizawa, M.; Kobayashi, T.; Akagi, K.; Shirikawa, H. *Phys. Rev. B* **1988**, *37*, 10301–10307.
- (6) Bredas, J.-L. L.; Cornil, J.; Heeger, A. J. *Adv. Mater.* **1996**, *8*, 447–452.
- (7) Rauscher, U.; Bassler, H.; Bradley, D.; Hennecke, M. *Phys. Rev. B* **1990**, *42*, 9830–9836.
- (8) Antoniadis, H.; Hsieh, B. R.; Abkowitz, M. A.; Jenekhe, S. A.; Stolka, M. *Mol. Cryst. Liq. Cryst. A* **1994**, *256*, 381–390.
- (9) Kepler, R. G.; Valencia, V. S.; Jacobs, S. J.; McNamara, J. J. *Synth. Met.* **1996**, *78*, 227–230.
- (10) Ferguson, A. J.; Kopidakis, N.; Shaheen, S. E.; Rumbles, G. J. *Phys. Chem. C* **2008**, *112*, 9865–9871.
- (11) Dicker, G.; Savenije, T. J.; Huisman, B.-H.; deLeeuw, D. M.; DeHaas, M. P.; Warman, J. M. *Synth. Met.* **2003**, *137*, 863–864.
- (12) Reid, O. G.; Rumbles, G. J. *Phys. Chem. Lett.* **2013**, *4*, 2348–2355.
- (13) Zaushtsyn, Y.; Gulbinas, V.; Zigmantas, D.; Zhang, F.; Inganäs, O.; Sundström, V.; Yartsev, A. *Phys. Rev. B* **2004**, *70*, 075202.
- (14) Reid, O. G.; Malik, J. A. N.; Latini, G.; Dayal, S.; Kopidakis, N.; Silva, C.; Stingelin, N.; Rumbles, G. J. *Polym. Sci. B Polym. Phys.* **2012**, *50*, 27–37.
- (15) Marsh, H. S.; Reid, O. G.; Barnes, G.; Heeney, M.; Stingelin, N.; Rumbles, G. J. *Polym. Sci. B Polym. Phys.*, submitted for publication.
- (16) Scholes, G. D.; Rumbles, G. *Nat. Mater.* **2006**, *5*, 683–696.
- (17) Bredas, J.-L. L.; Beljonne, D.; Coropceanu, V.; Cornil, J. *Chem. Rev.* **2004**, *104*, 4971–5004.
- (18) Spano, F. C. *Acc. Chem. Res.* **2010**, *43*, 429–439.
- (19) Scholes, G. D. *Acc. Nano* **2008**, *2*, 523–537.
- (20) Harcourt, R. D.; Scholes, G. D.; Ghiggino, K. P. *J. Chem. Phys.* **1994**, *101*, 10521.
- (21) McGlynn, S. P.; Armstrong, A. T.; Azumi, T. In *Modern Quantum Chemistry*; Sinanoglu, O., Ed.; Academic Press: New York, 1965; Vol. 111, p 203.
- (22) Scholes, G. D.; Ghiggino, K. P. *J. Phys. Chem.* **1994**, *98*, 4580–4590.
- (23) Rettig, W.; Zander, M. *Ber. Bunsen-Ges. Phys. Chem.* **1983**, *87*, 1143–1149.
- (24) Mataga, N.; Yao, H.; Okada, T.; Rettig, W. J. *Phys. Chem.* **1989**, *93*, 3383–3386.
- (25) Kang, T. J.; Jarzeba, W.; Barbara, P. F.; Fonseca, T. *Chem. Phys.* **1990**, *149*, 81–95.
- (26) Scholes, G. D.; Fournier, T.; Parker, A. W.; Phillips, D. J. *Chem. Phys.* **1999**, *111*, 5999.
- (27) Conwell, E. M. *Synth. Met.* **1997**, *85*, 995–999.
- (28) Aryanpour, K.; Sheng, C. X.; Olejnik, E.; Pandit, B.; Psichos, D.; Mazumdar, S.; Vardeny, Z. V. *Phys. Rev. B* **2011**, *83*, 155124.
- (29) Hsu, J.; Yan, M.; Jedju, T.; Rothberg, L. J.; Hsieh, B. R. *Phys. Rev. B* **1994**, *49*, 712–715.
- (30) Sheng, C. X.; Tong, M.; Singh, S.; Vardeny, Z. V. *Phys. Rev. B* **2007**, *75*, 085206.
- (31) Hodgkiss, J. M.; Albert-Seifried, S.; Rao, A.; Barker, A. J.; Campbell, A. R.; Marsh, R. A.; Friend, R. H. *Adv. Func. Mater.* **2012**, *22*, 1567–1577.
- (32) Gélinas, S.; Kirkpatrick, J.; Howard, I. A.; Johnson, K.; Wilson, M. W. B.; Pace, G.; Friend, R. H.; Silva, C. J. *Phys. Chem. B* **2013**, *117*, 4649–4653.
- (33) Piris, J.; Dykstra, T. E.; Bakulin, A. A.; van Loosdrecht, P. H. M.; Knulst, W.; Trinh, M. T.; Schins, J. M.; Siebbeles, L. D. A. *J. Phys. Chem. C* **2009**, *113*, 14500–14506.
- (34) Gulbinas, V.; Zaushtsyn, Y.; Sundström, V.; Hertel, D.; Bassler, H.; Yartsev, A. *Phys. Rev. Lett.* **2002**, *89*, 107401.
- (35) Marsh, R. A.; Hodgkiss, J. M.; Albert-Seifried, S.; Friend, R. H. *Nano Lett.* **2010**, *10*, 923–930.
- (36) Silva, C.; Dhoot, A.; Russell, D.; Stevens, M.; Arias, A.; MacKenzie, J.; Greenham, N.; Friend, R. H.; Setayesh, S.; Müllen, K. *Phys. Rev. B* **2001**, *64*, 125211.
- (37) Köhler, A.; Dos Santos, D.; Beljonne, D.; Shuai, Z.; Bredas, J.-L. L.; Holmes, A. B.; Kraus, A.; Müllen, K.; Friend, R. H. *Nature* **1998**, *392*, 903–906.
- (38) Bredas, J.-L. L.; Cornil, J.; Beljonne, D.; Dos Santos, D. A.; Shuai, Z. *Acc. Chem. Res.* **1999**, *32*, 267–276.
- (39) Martini, I.; Smith, A.; Schwartz, B. J. *Phys. Rev. B* **2004**, *69*, 035204.
- (40) Denton, G. J.; Tessler, N.; Stevens, M. A.; Friend, R. H. *Synth. Met.* **1999**, *102*, 1008–1009.
- (41) Mizes, H. A.; Conwell, E. M. *Phys. Rev. B* **1994**, *50*, 11243–11246.
- (42) Su, W. P.; Schrieffer, J. R.; Heeger, A. J. *Phys. Rev. B* **1980**, *22*, 2099.
- (43) Heeger, A. J. In *Primary Photoexcitations in Conjugated Polymers: Molecular Exciton versus Semiconductor Band Model*; Sariciftci, N. S., Ed.; World Scientific Publishing: Hackensack, NJ, 1997.
- (44) Kersting, R.; Lemmer, U.; Deussen, M.; Bakker, H.; Mahrt, R.; Kurz, H.; Arkhipov, V.; Bassler, H.; Göbel, E. *Phys. Rev. Lett.* **1994**, *73*, 1440–1443.
- (45) Conwell, E. M.; Mizes, H. A. *Phys. Rev. B* **1995**, *51*, 6953–6958.
- (46) Hendry, E.; Schins, J.; Candeias, L.; Siebbeles, L. D. A.; Bonn, M. *Phys. Rev. Lett.* **2004**, *92*, 196601.
- (47) Hendry, E.; Koeberg, M.; Schins, J.; Siebbeles, L. D. A.; Bonn, M. *Chem. Phys. Lett.* **2006**, *432*, 441–445.
- (48) Hendry, E.; Koeberg, M.; Schins, J.; Nienhuys, H.; Sundström, V.; Siebbeles, L. D. A.; Bonn, M. *Phys. Rev. B* **2005**, *71*, 125201.
- (49) Yan, M.; Rothberg, L. J.; Papadimitrakopoulos, F.; Galvin, M.; Miller, T. *Phys. Rev. Lett.* **1994**, *72*, 1104–1107.
- (50) Lane, P. A.; Wei, X.; Vardeny, Z. V. *Phys. Rev. B* **1997**, *56*, 4626.
- (51) Frankevich, E.; Ishii, H.; Hamaoka, Y.; Yokoyama, T.; Fuji, A.; Li, S.; Yoskino, K.; Nakamura, A.; Seki, K. *Phys. Rev. B* **2000**, *62*, 2505–2515.
- (52) Müller, J.; Lemmer, U.; Feldmann, J.; Scherf, U. *Phys. Rev. Lett.* **2002**, *88*, 147401.
- (53) Yan, M.; Rothberg, L. J.; Kwock, E.; Miller, T. *Phys. Rev. Lett.* **1995**, *75*, 1992–1995.
- (54) Jenekhe, S. A.; Osaheni, J. A. *Science* **1994**, *265*, 765–768.
- (55) Jakubiak, R.; Collison, C. J.; Wan, W. C.; Rothberg, L. J.; Hsieh, B. R. *J. Phys. Chem. A* **1999**, *103*, 2394–2398.
- (56) Nguyen, T.-Q.; Martini, I. B.; Liu, J.; Schwartz, B. J. *J. Phys. Chem. B* **2000**, *104*, 237–255.
- (57) Schaller, R. D.; Lee, L. F.; Johnson, J. C.; Haber, L. H.; Saykally, R. J.; Viece, J.; Benjamin, I.; Nguyen, T.-Q.; Schwartz, B. J. *J. Phys. Chem. B* **2002**, *106*, 9496–9506.
- (58) Mahrt, R. F.; Pauck, T.; Lemmer, U.; Siegner, U.; Hopmeier, M.; Hennig, R.; Bassler, H.; Göbel, E. O.; Bolivar, P. H.; Wegmann, G. *Phys. Rev. B* **1996**, *54*, 1759.

- (59) Schwartz, B. J. *Annu. Rev. Phys. Chem.* **2003**, *54*, 141–172.
- (60) Ogilvie, J. P.; Kubarych, K. J. In *Advances In Atomic, Molecular, and Optical Physics*; Arimondo, E.; Berman, P. R.; Lin, C. C., Eds.; Elsevier: New York, 2009; Vol. 57, pp 1–444.
- (61) Collini, E.; Scholes, G. D. *Science* **2009**, *323*, 369–373.
- (62) Collini, E.; Scholes, G. D. *J. Phys. Chem. A* **2009**, *113*, 4223–4241.
- (63) Hwang, I.; Beaupré, S.; Leclerc, M.; Scholes, G. D. *Chem. Sci.* **2012**, *3*, 2270.
- (64) Anna, J. M.; Song, Y.; Dinshaw, R.; Scholes, G. D. *Pure Appl. Chem.* **2013**, *85*, 1307–1319.
- (65) Mukamel, S. *Annu. Rev. Phys. Chem.* **2000**, *51*, 691–729.
- (66) Jonas, D. M. *Annu. Rev. Phys. Chem.* **2003**, *54*, 425–463.
- (67) Hochstrasser, R. M. *Proc. Natl. Acad. Sci. U.S.A.* **2007**, *104*, 14190–14196.
- (68) Cho, M. *Chem. Rev.* **2008**, *108*, 1331–1418.
- (69) Abramavicius, D.; Palmieri, B.; Voronine, D. V.; Šanda, F.; Mukamel, S. *Chem. Rev.* **2009**, *109*, 2350–2408.
- (70) Cho, M. *Two-Dimensional Optical Spectroscopy*; CRC Press: Boca Raton, FL, 2009.
- (71) Hama, P.; Zanni, M. T. *Concepts and Methods of 2D Infrared Spectroscopy*; Cambridge University Press: Cambridge, 2011.
- (72) Hukic-Markosian, G.; Basel, T.; Singh, S.; Vardeny, Z. V.; Li, S.; Laird, D. *Appl. Phys. Lett.* **2012**, *100*, 213903–213905.
- (73) Osterbacka, R.; An, C. P.; Jiang, X. M.; Vardeny, Z. V. *Science* **2000**, *287*, 839–842.
- (74) Guo, J.; Ohkita, H.; Bente, H.; Ito, S. *J. Am. Chem. Soc.* **2009**, *131*, 16869–16880.
- (75) Guo, J.; Ohkita, H.; Bente, H.; Ito, S. *J. Am. Chem. Soc.* **2010**, *132*, 6154–6164.
- (76) Samuel, I. D. W.; Rumbles, G.; Friend, R. H. In *Primary Photoexcitations in Conjugated Polymers: Molecular Exciton versus Semiconductor Band Model*; Sariciftci, N. S., Ed.; World Scientific Publishing: Hackensack, NJ, 1997.
- (77) Tekavec, P. F.; Myers, J. A.; Lewis, K. L. M.; Ogilvie, J. P. *Opt. Lett.* **2009**, *34*, 1390–1392.
- (78) Tyagi, P.; Saari, J. I.; Walsh, B.; Kabir, A.; Crozatier, V.; Forget, N.; Kambhampati, P. *J. Phys. Chem. A* **2013**, *117*, 6264–6269.
- (79) Brida, D.; Manzoni, C.; Cerullo, G. *Opt. Lett.* **2012**, *37*, 3027–3029.
- (80) Jiang, X.; Osterbacka, R.; Korovyanko, O.; An, C.; Horovitz, B.; Janssen, R. A.; Vardeny, Z. V. *Adv. Func. Mater.* **2002**, *12*, 587–597.
- (81) Korovyanko, O.; Osterbacka, R.; Jiang, X.; Vardeny, Z. V.; Janssen, R. A. *Phys. Rev. B* **2001**, *64*, 235122.
- (82) Miller, P. F.; de Souza, M. M.; Moratti, S. C.; Holmes, A. B.; Samuel, I. D.; Rumbles, G. *Polym. Int.* **2006**, *55*, 784–792.
- (83) Dicker, G.; de Haas, M. P.; Siebbeles, L. D. A.; Warman, J. M. *Phys. Rev. B* **2004**, *70*, 045203.
- (84) Paquin, F.; Latini, G.; Sakowicz, M.; Karsenti, P.-L.; Wang, L.; Beljonne, D.; Stingelin, N.; Silva, C. *Phys. Rev. Lett.* **2011**, *106*, 197401.
- (85) Rothberg, L. J.; Van, M.; Fung, A.; Jedju, T. M.; Kwock, E. W.; Galvin, M. E. *Synth. Met.* **1997**, *84*, 537–538.
- (86) Bakulin, A. A.; Rao, A.; Pavelyev, V. G.; van Loosdrecht, P. H. M.; Pshenichnikov, M. S.; Niedzialek, D.; Cornil, J.; Beljonne, D.; Friend, R. H. *Science* **2012**, *335*, 1340–1344.
- (87) Graupner, W.; Cerullo, G.; Lanzani, G.; Nisoli, M.; List, E.; Leising, G.; De Silvestri, S. *Phys. Rev. Lett.* **1998**, *81*, 3259.
- (88) Gulbinas, V.; Zaushtsyn, Y.; Bassler, H.; Yartsev, A.; Sundström, V. *Phys. Rev. B* **2004**, *70*, 035215.
- (89) Scheblykin, I. G.; Yartsev, A.; Pullerits, T.; Gulbinas, V.; Sundström, V. *J. Phys. Chem. B* **2007**, *111*, 6303–6321.
- (90) Meng, H.-F.; Hong, T.-M. *Phys. Rev. B* **2000**, *61*, 9913.
- (91) Harrison, M.; Grüner, J.; Spencer, G. *Phys. Rev. B* **1997**, *55*, 7831–7849.
- (92) Dicker, G. *Photogeneration and Dynamics of Charge Carriers in the Conjugated polymer poly(3-hexylthiophene)*; Technische Universiteit Delft: Delft, The Netherlands, 2004; pp 1–144.
- (93) Gettinger, C. L.; Heeger, A. J.; Drake, J. M.; Pine, D. J. *J. Chem. Phys.* **1994**, *101*, 1673.
- (94) He, G.; Li, Y.; Liu, J.; Yang, Y. *Appl. Phys. Lett.* **2002**, *80*, 4247.
- (95) Nguyen, T.-Q.; Kwong, R. C.; Thompson, M. E.; Schwartz, B. J. *Synth. Met.* **2001**, *119*, 523–524.
- (96) Hwang, I.; Scholes, G. D. *Chem. Mater.* **2011**, *23*, 610–620.
- (97) Collison, C. J.; Rothberg, L. J.; Treemanekarn, V.; Li, Y. *Macromolecules* **2001**, *34*, 2346–2352.
- (98) Yu, J. *Science* **2000**, *289*, 1327–1330.
- (99) Köhler, A.; Hoffmann, S. T.; Bassler, H. *J. Am. Chem. Soc.* **2012**, *134*, 11594–11601.
- (100) M, H.; Kasha, M. *Photochem. Photobiol.* **1964**, *3*, 317–331.
- (101) Kasha, M. *Radiat. Res.* **1963**, *20*, 55–71.
- (102) Martin, T. P.; Wise, A. J.; Busby, E.; Gao, J.; Roehling, J. D.; Ford, M. J.; Larsen, D. S.; Moulé, A. J.; Grey, J. K. *J. Phys. Chem. B* **2013**, *117*, 4478–4487.
- (103) Lécuyer, R.; Berréhar, J.; Ganière, J.; Lapersonne-Meyer, C.; Lavallard, P.; Schott, M. *Phys. Rev. B* **2002**, *66*, 125205.
- (104) Clark, J.; Silva, C.; Friend, R. H.; Spano, F. C. *Phys. Rev. Lett.* **2007**, *98*, 206406.
- (105) Niles, E. T.; Roehling, J. D.; Yamagata, H.; Wise, A. J.; Spano, F. C.; Moulé, A. J.; Grey, J. K. *J. Phys. Chem. Lett.* **2012**, *259*–263.
- (106) Spano, F. C. *J. Chem. Phys.* **2005**, *122*, 234701.
- (107) Spano, F. C. *Annu. Rev. Phys. Chem.* **2006**, *57*, 217–243.
- (108) Fidler, H.; Knoester, J.; Wiersma, D. A. *J. Chem. Phys.* **1991**, *95*, 7880.
- (109) Cornil, J.; Beljonne, D.; Shu, Z.; Hagler, T. W.; Campbell, I.; Bradley, D.; Bredas, J.-L. L.; Spangler, C. W.; Mullen, K. *Chem. Phys. Lett.* **1995**, *247*, 425–432.
- (110) Cornil, J.; Heeger, A. J.; Bredas, J.-L. L. *Chem. Phys. Lett.* **1997**, *272*, 463–470.
- (111) Cornil, J.; Dos Santos, D. A.; Crispin, X.; Silbey, R.; Bredas, J.-L. L. *J. Am. Chem. Soc.* **1998**, *120*, 1289–1299.
- (112) Cornil, J.; Beljonne, D.; Calbert, J. P.; Bredas, J.-L. L. *Adv. Mater.* **2001**, *13*, 1053–1067.
- (113) Beljonne, D.; Cornil, J.; Silbey, R.; Millié, P.; Bredas, J.-L. L. *J. Chem. Phys.* **2000**, *112*, 4749–4758.
- (114) Halls, J.; Cornil, J.; Dos Santos, D. A.; Silbey, R.; Hwang, D.-H.; Holmes, A. B.; Bredas, J.-L. L.; Friend, R. H. *Phys. Rev. B* **1999**, *60*, 5721.
- (115) Mueller, C.; Zhigadlo, N. D.; Kumar, A.; Baklar, M. A.; Karpinski, J.; Smith, P.; Kreouzis, T.; Stingelin, N. *Macromolecules* **2011**, *44*, 1221–1225.
- (116) Virkar, A. A.; Mannsfeld, S.; Bao, Z.; Stingelin, N. *Adv. Mater.* **2010**, *22*, 3857–3875.
- (117) Stingelin, N. *Polym. Int.* **2012**, *61*, 866–873.
- (118) Koch, F. P. V.; Rivnay, J.; Foster, S.; Müller, C.; Downing, J.; Buchaca-Domingo, E.; Westacott, P.; Yu, L.; Yuan, M.; Baklar, M.; Fei, Z.; Luscombe, C.; McLachlan, M. A.; Heeney, M.; Rumbles, G.; Silva, C.; Salleo, A.; Nelson, J.; Smith, P.; Stingelin, N. *Prog. Polym. Sci.* **2013**, DOI: 10.1016/j.progpolymsci.2013.07.009.
- (119) Noriega, R.; Rivnay, J.; Vandewal, K.; Koch, F. P. V.; Stingelin, N.; Smith, P.; Toney, M. F.; Salleo, A. *Nat. Mater.* **2013**, DOI: 10.1038/nmat3722.
- (120) Treat, N. D.; Nekuda Malik, J. A.; Reid, O. G.; Yu, L.; Shuttle, C. G.; Rumbles, G.; Hawker, C. J.; Chabiny, M. L.; Smith, P.; Stingelin, N. *Nat. Mater.* **2013**, *12*, 628–633.
- (121) Brinkmann, M.; Rannou, P. *Adv. Func. Mater.* **2007**, *17*, 101–108.
- (122) Brinkmann, M.; Rannou, P. *Macromolecules* **2009**, *42*, 1125–1130.
- (123) Brinkmann, M. *J. Polym. Sci. B Polym. Phys.* **2011**, *49*, 1218–1233.
- (124) Liu, J.; Arif, M.; Zou, J.; Khondaker, S. I.; Zhai, L. *Macromolecules* **2009**, *42*, 9390–9393.
- (125) Kim, F. S.; Ren, G.; Jenekhe, S. A. *Chem. Mater.* **2011**, *23*, 682–732.
- (126) Lim, J. A.; Liu, F.; Ferdous, S.; Muthukumar, M.; Briseno, A. L. *Mater. Today* **2010**, *13*, 14–24.
- (127) Kline, R. J.; McGehee, M. D.; Kadnikova, E. N.; Liu, J.; Fréchet, J. M. J.; Toney, M. F. *Macromolecules* **2005**, *38*, 3312–3319.



- (128) Zhang, R.; Li, B.; Iovu, M. C.; Jeffries-EL, M.; Sauv  , G.; Cooper, J.; Jia, S.; Tristram-Nagle, S.; Smilgies, D. M.; Lambeth, D. N.; McCullough, R. D.; Kowalewski, T. *J. Am. Chem. Soc.* **2006**, *128*, 3480–3481.
- (129) Tong, M.; Cho, S.; Rogers, J. T.; Schmidt, K.; Hsu, B. B. Y.; Moses, D.; Coffin, R. C.; Kramer, E. J.; Bazan, G. C.; Heeger, A. J. *Adv. Func. Mater.* **2010**, *20*, 3959–3965.
- (130) Chang, J.-F.; Clark, J.; Zhao, N.; Sirringhaus, H.; Breiby, D. W.; Andreasen, J. W.; Nielsen, M. M.; Giles, M.; Heeney, M.; McCulloch, I. *Phys. Rev. B* **2006**, *74*, 115318.
- (131) Ungar, G.; Stejny, J.; Keller, A.; Bidd, I.; Whiting, M. C. *Science* **1985**, *229*, 386–389.
- (132) Keller, A. *Rep. Prog. Phys.* **1968**, *31*, 623.
- (133) Ungar, G.; Zeng, X.-B. *Chem. Rev.* **2001**, *101*, 4157–4188.
- (134) Wunderlich, B. *Macromolecular Physics, Vol. 1. Structure, Morphology, Defects*; Academic Press: London, 1973.
- (135) Xin, H.; Reid, O. G.; Ren, G.; Kim, F. S.; Ginger, D. S.; Jenekhe, S. A. *ACS Nano* **2010**, *4*, 1861–1872.
- (136) Roehling, J. D.; Arslan, I.; Moul  , A. J. *J. Mater. Chem.* **2012**, *22*, 2498–2506.
- (137) Berson, S.; de Bettignies, R.; Bailly, S.; Guillerez, S. *Adv. Func. Mater.* **2007**, *17*, 1377–1384.
- (138) Keg, P.; Lohani, A.; Fichou, D.; Lam, Y. M.; Wu, Y.; Ong, B. S.; Mhaisalkar, S. G. *Macromol. Rapid Commun.* **2008**, *29*, 1197–1202.
- (139) Gr  vin, B.; Rannou, P.; Payerne, R.; Pron, A.; Travers, J. P. *Adv. Mater.* **2003**, *15*, 881–884.
- (140) Gr  vin, B.; Rannou, P.; Payerne, R.; Pron, A.; Travers, J. P. *J. Chem. Phys.* **2003**, *118*, 7097.
- (141) Mena Osteritz, E.; Meyer, A.; Langeveld Voss, B. M.; Janssen, R. A.; Meijer, E. W.; B  uerle, P. *Angew. Chem.* **2000**, *112*, 2791–2796.
- (142) Zhang, X.; Bronstein, H.; Kronemeijer, A. J.; Smith, J.; Kim, Y.; Kline, R. J.; Richter, L. J.; Anthopoulos, T. D.; Sirringhaus, H.; Song, K.; Heeney, M.; Zhang, W.; McCulloch, I.; DeLongchamp, D. M. *Nat. Comm.* **2013**, *4*, 2238.
- (143) Pingel, P.; Zen, A.; Abell  n, R. D.; Grozema, F. C.; Siebbeles, L. D. A.; Neher, D. *Adv. Func. Mater.* **2010**, *20*, 2286–2295.
- (144) Osterbacka, R.; Genevi  cius, K.; Pivrikas, A.; Ju  ska, G.; Arlauskas, K.; Kreouzis, T.; Bradley, D. D. C.; Stubbs, H. *Synth. Met.* **2003**, *139*, 811–813.
- (145) Kitamura, C.; Tanaka, S.; Yamashita, Y. *Chem. Mater.* **1996**, *8*, 570–578.
- (146) Bundgaard, E.; Krebs, F. *Solar Energy Mater. Solar Cells* **2007**, *91*, 954–985.
- (147) Blouin, N.; Michaud, A.; Leclerc, M. *Adv. Mater.* **2007**, *19*, 2295–2300.
- (148) Zou, Y.; Najari, A.; Berrouard, P.; Beaupr  , S.; R  da A  ch, B.; Tao, Y.; Leclerc, M. *J. Am. Chem. Soc.* **2010**, *132*, 5330–5331.
- (149) Liang, Y.; Wu, Y.; Feng, D.; Tsai, S.-T.; Son, H. J.; Li, G.; Yu, L. *J. Am. Chem. Soc.* **2009**, *131*, 56–57.
- (150) Liang, Y.; Feng, D.; Wu, Y.; Tsai, S.-T.; Li, G.; Ray, C.; Yu, L. *J. Am. Chem. Soc.* **2009**, *131*, 7792–7799.
- (151) He, Z.; Zhong, C.; Su, S.; Xu, M.; Wu, H.; Cao, Y. *Nat. Photon.* **2012**, *6*, 593–597.
- (152) You, J.; Dou, L.; Yoshimura, K.; Kato, T.; Ohya, K.; Moriarty, T.; Emery, K.; Chen, C.-C.; Gao, J.; Li, G.; Yang, Y. *Nat. Comm.* **2013**, *4*, 1446.
- (153) Jespersen, K. G.; Beenken, W. J. D.; Zaushtsyn, Y.; Yartsev, A.; Andersson, M.; Pullerits, T.; Sundstr  m, V. *J. Chem. Phys.* **2004**, *121*, 12613.
- (154) Banerji, N.; Gagnon, E.; Morgantini, P.-Y.; Valouch, S.; Mohebbi, A. R.; Seo, J. H.; Leclerc, M.; Heeger, A. J. *J. Phys. Chem. C* **2012**, *116*, 11456–11469.
- (155) Gieseke, B.; J  ck, B.; Preis, E.; Jung, S.; Forster, M.; Scherf, U.; Deibel, C.; Dyakonov, V. *Adv. Energy Mater.* **2012**, *2*, 1477–1482.
- (156) Carsten, B.; Szarko, J. M.; Son, H. J.; Wang, W.; Lu, L.; He, F.; Rolczynski, B. S.; Lou, S. J.; Chen, L. X.; Yu, L. *J. Am. Chem. Soc.* **2011**, *133*, 20468–20475.
- (157) Tautz, R.; Da Como, E.; Limmer, T.; Feldmann, J.; Egelhaaf, H.-J.; von Hauff, E.; Lema  ur, V.; Beljonne, D.; Yilmaz, S.; Dumsch, I.; Allard, S.; Scherf, U. *Nat. Comm.* **2012**, *3*, 970.
- (158) Rolczynski, B. S.; Szarko, J. M.; Son, H. J.; Liang, Y.; Yu, L.; Chen, L. X. *J. Am. Chem. Soc.* **2012**, *134*, 4142–4152.
- (159) Szarko, J. M.; Rolczynski, B. S.; Lou, S. J.; Xu, T. *Adv. Func. Mater.* **2013**, DOI: 10.1002/adfm.201301820.
- (160) Johnson, K.; Huang, Y.-S.; Huettner, S.; Sommer, M.; Brinkmann, M.; Mulherin, R.; Niedzialek, D.; Beljonne, D.; Clark, J.; Huck, W. T. S.; Friend, R. H. *J. Am. Chem. Soc.* **2013**, *135*, 5074–5083.
- (161) Di Nuzzo, D.; Wetzelaer, G.-J. A. H.; Bouwer, R. K. M.; Gevaerts, V. S.; Meskers, S. C. J.; Hummelen, J. C.; Blom, P. W. M.; Janssen, R. A. *Adv. Energy Mater.* **2012**, *3*, 85–94.
- (162) Graham, K. R.; Erwin, P.; Nordlund, D.; Vandewal, K.; Li, R.; Ngongang Ndjawa, G. O.; Hoke, E. T.; Salleo, A.; Thompson, M. E.; McGehee, M. D.; Amassian, A. *Adv. Mater.* **2013**, DOI: 10.1002/adma.201301319.
- (163) Camaioni, N.; Po, R. *J. Phys. Chem. Lett.* **2013**, 1821–1828.
- (164) Servaites, J. D.; Savoie, B. M.; Brink, J. B.; Marks, T. J.; Ratner, M. A. *Energy Environ. Sci.* **2012**, *5*, 8343–8350.
- (165) Tsang, S.-W.; Chen, S.; So, F. *Adv. Mater.* **2013**, *25*, 2434–2439.
- (166) Faist, M. A.; Shoaee, S.; Tuladhar, S.; Dibb, G. F.; Foster, S.; Gong, W.; Kirchartz, T.; Bradley, D. D.; Durrant, J. R.; Nelson, J. *Adv. Energy Mater.* **2013**, *3*, 744–752.
- (167) Janssen, R. A.; Nelson, J. *Adv. Mater.* **2013**, *25*, 1847–1858.
- (168) Vandewal, K.; Ma, Z.; Bergqvist, J.; Tang, Z.; Wang, E.; Henriksson, P.; Tvingstedt, K.; Andersson, M. R.; Zhang, F.; Ingan  s, O. *Adv. Func. Mater.* **2012**, *22*, 3480–3490.
- (169) van der Hofstad, T. G.; Di Nuzzo, D.; van den Berg, M.; Janssen, R. A.; Meskers, S. C. *Adv. Energy Mater.* **2012**, *2*, 1095–1099.
- (170) Rance, W. L.; Ferguson, A. J.; McCarthy-Ward, T.; Heeney, M.; Ginley, D. S.; Olson, D. C.; Rumbles, G.; Kopidakis, N. *ACS Nano* **2011**, *5*, 5635–5646.
- (171) Wodo, O.; Roehling, J. D.; Moul  , A. J. *Energy Environ. Sci.* **2013**, DOI: 10.1039/c3ee41224e.
- (172) Collins, B. A.; Tumbleston, J. R.; Ade, H. *J. Phys. Chem. Lett.* **2011**, *2*, 3135–3145.
- (173) Pfannm  ller, M.; Fl  gge, H.; Benner, G.; Wacker, I.; Sommer, C.; Hanselmann, M.; Schmale, S.; Schmidt, H.; Hamprecht, F. A.; Rabe, T.; Kowalsky, W.; Schr  der, R. R. *Nano Lett.* **2011**, *11*, 3099–3107.
- (174) Kandada, A. R. S.; Grancini, G.; Petrozza, A.; Perissinotto, S.; Fazzi, D.; Raavi, S. S. K.; Lanzani, G. *Sci. Rep.* **2013**, *3*, 2073.